

1 *Bifidobacterium longum* modifies a nutritional intervention for stunting in Zimbabwean infants

2 Authors: Ethan K Gough^{1,*}, Thaddeus J Edens², Lynnea Carr³, Ruairi C Robertson⁴, Kuda Mutasa⁵, Robert
3 Ntozini⁵, Bernard Chasekwa⁵, Hyun Min Geum⁶, Iman Baharmand⁶, Sandeep K Gill⁶, Batsirai Mutasa⁵,
4 Mduduzi N N Mbuya^{5,7}, Florence D Majo⁵, Naume Tavengwa⁵, Freddy Francis⁸, Joice Tome⁵, Ceri
5 Evans^{4,5,9}, Margaret Kosek¹⁰, Andrew J Prendergast^{4,5}, Ameer R Manges^{6,11} for the Sanitation Hygiene
6 Infant Nutrition Efficacy (SHINE) Trial Team.

7 Affiliations:

8 ¹Department of International Health, Johns Hopkins Bloomberg School of Public Health, Baltimore, MD,
9 21205, USA.

10 ²Devil's Staircase Consulting, West Vancouver, BC, Canada.

11 ³Department of Microbiology and Immunology, University of British Columbia, Vancouver, BC, V6T 1Z3,
12 Canada.

13 ⁴Blizard Institute, Queen Mary University of London, London, E1 2AT, UK.

14 ⁵Zvitambo Institute for Maternal and Child Health Research, Harare, Zimbabwe.

15 ⁶School of Population and Public Health, University of British Columbia, Vancouver, BC, V6T 1Z3, Canada.

16 ⁷Global Alliance for Improved Nutrition, Washington, DC, 20036, USA.

17 ⁸Department of Experimental Medicine, University of British Columbia, Vancouver, BC, V6T 1Z2, Canada.

18 ⁹Department of Clinical Infection, Microbiology and Immunology, University of Liverpool, Liverpool, L69
19 3BX, UK

20 ¹⁰University of Virginia School of Medicine, Charlottesville, VA, USA.

21 ¹¹British Columbia Centre for Disease Control (BCCDC), Vancouver, BC, Canada.

22 *Correspondence: egough1@jh.edu

23

24

25

26

27

28

29

30

31

32

33

34

35

36

37

38

39

40 **Summary**

41 Child stunting is an indicator of chronic undernutrition and reduced human capital. Small-quantity lipid-
42 based nutrient supplements (SQ-LNS) has been widely tested to reduce stunting, but has modest effects.
43 The infant intestinal microbiome may contribute to stunting, and is partly shaped by mother and infant
44 histo-blood group antigens (HBGA). We investigated whether mother-infant fucosyltransferase status,
45 which governs HBGA, and the infant gut microbiome modified the impact of SQ-LNS on stunting at age
46 18 months among Zimbabwean infants in the SHINE Trial (NCT01824940). We found that mother-infant
47 fucosyltransferase discordance and *Bifidobacterium longum* modified SQ-LNS efficacy. Infant age-related
48 microbiome shifts in *B. longum* subspecies dominance from *infantis*, a proficient human milk
49 oligosaccharide utilizer, to *suis* or *longum*, proficient plant-polysaccharide utilizers, were partly
50 influenced by discordance in mother-infant FUT2+/FUT3- phenotype, suggesting that a “younger”
51 microbiome at initiation of SQ-LNS reduces its benefits on stunting in areas with a high prevalence of
52 linear growth restriction.

53

54 Keywords: microbiome, nutrition, fucosyltransferase, histo-blood group antigen, stunting, infant

55

56

57

58

59

60

61 Introduction

62 Globally, 21% of children under 5 years of age (149 million) are stunted¹, defined as having a length
63 or height >2 standard deviations below an age- and sex-matched reference population median². Deficits
64 in linear growth largely accrue from conception to 24 months of age^{3,4}, corresponding to the period
65 when normal child growth and development is most rapid. Stunting is associated with reductions in child
66 survival, neurodevelopment, educational attainment, and adult economic productivity⁵⁻⁷.

67 A broadly tested intervention to reduce stunting has been provision of small-quantity lipid-based
68 nutrient supplements (SQ-LNS) to improve infant and young child feeding (IYCF) starting at 6-months
69 (mo) of age, which is the recommended time for introduction of complementary foods. Randomized
70 controlled trials (RCT) of SQ-LNS provision to infants have shown small reductions in stunting (12%
71 relative reduction), but effects have varied^{8,9}. Evidence to support other nutrition interventions, which
72 address the underlying determinants of stunting during the first 1000 days of life, starting from
73 conception, is also limited¹⁰. Elucidating the reasons for the limited impact of nutritional interventions
74 that are designed to alleviate stunting is crucial to the development of more effective strategies.

75 Recently, the human microbiome has been shown to impact infant health¹¹, and studies suggest a
76 role of the intestinal microbiome in child growth, particularly ponderal growth^{12,13}. The prevailing view
77 holds that intestinal colonization with bacteria begins at birth, after which the microbiome progresses
78 through a succession of identifiable shifts in composition and functional capacity¹¹ that correspond
79 closely with infant age and developmental stage¹⁴. Deviations from an age-appropriate composition may
80 be associated with poor health outcomes¹⁴⁻¹⁷, including undernutrition in low resource settings^{14,18-20}.
81 However, results vary²¹⁻²⁵ and evidence for a causal effect of the intestinal microbiome on growth
82 comes predominantly from animal models. In these experiments, a combination of commensal bacteria
83 and a nutrient-poor diet produce a synergistic effect on growth faltering. The detrimental effect on

84 growth was worse when certain commensal bacteria, which can act as pathobionts (e.g. *Bacteroides*
85 *thetaiotaomicron* and *Bacteroides fragilis*), were present in the gut along with pathogenic species^{26,27}.

86 The gut microbiome in infants is influenced by breastfeeding, with differences persisting beyond age
87 6mo¹⁶. Breastfeeding-associated differences are partly driven by differences in human milk
88 oligosaccharide (HMO) composition, which are metabolized by specific commensal bacteria and thereby
89 influence the growth and activity of bacterial populations in the infant gut, in particular,
90 *Bifidobacterium*^{28,29}. In addition, HMOs in combination with commensal gut bacteria have been shown
91 to improve growth in animal models of undernutrition³⁰. Active maternal α -1,2-fucosyltransferase
92 (FUT2) and α -1,3-fucosyltransferase (FUT3) genes are key determinants of HMO composition³¹⁻³³. These
93 genes encode enzymes which catalyze addition of fucose to the disaccharides that serve as precursors to
94 host glycan production^{34,35}. Individuals with at least one functional FUT2 or FUT3 allele produce
95 fucosylated histo-blood group antigens (HBGA) and are called “secretors” or “Lewis-positive”,
96 respectively;³⁵ by contrast, individuals lacking two functional FUT2 or FUT3 alleles don’t produce
97 fucosylated HBGAs, and are termed “non-secretors” or “Lewis-null”, respectively³⁵. These secretor and
98 Lewis phenotypes act in concert to synthesize a variety of HBGAs (Figure S1)^{34,35}. In addition to the
99 impact of maternal FUT2 or FUT3 status on the infant gut microbiome via their influence on HMO
100 composition, host FUT2 and FUT3 phenotypes also determine tissue surface HBGA expression in the gut,
101 which may also affect the microbiome through the availability host glycans and competition for
102 adhesion sites³⁶⁻⁴⁰.

103 There is growing interest in the moderating effect of the gut microbiome on nutritional
104 interventions. Recent RCTs showed that the impact of dietary interventions for weight reduction on
105 metabolic health outcomes is modified up to 4-fold by microbiota composition⁴¹⁻⁴⁴. Effect modification
106 of host diet by the gut microbiota has also been investigated in observational studies, which report that
107 microbiome composition modified the association between diet and biomarkers of metabolic syndrome

108 by up to 2-fold⁴⁵⁻⁴⁷. Gut microbiota composition, therefore, may also be an important modifier of dietary
109 interventions on infant health. Only one study to date investigated the gut microbiota as an effect
110 modifier of SQ-LNS on infant stunting, and reported limited evidence of effect-modification⁴⁸. However,
111 several studies have reported a synergistic effect of microbiome composition and diet on undernutrition
112 phenotypes using animal models^{26,27,49,50}.

113 Here we aimed to determine the effect of infant gut microbiome composition and functional
114 capacity on efficacy of an IYCF intervention that included SQ-LNS to reduce stunting (primary outcome)
115 and improve length-for-age z-score (LAZ) (secondary outcome) at age 18mo. We hypothesized that the
116 efficacy of IYCF, when started at age 6mo, on infant linear growth is modified by mother and infant FUT2
117 and FUT3 phenotype, as an drivers of variation in gut microbiome composition, and by the infant gut
118 microbiome. We tested this hypothesis using data from HIV-unexposed infants enrolled in the Sanitation
119 Hygiene Infant Nutrition Efficacy (SHINE) trial conducted in rural Zimbabwe, in which the IYCF
120 intervention modestly increased LAZ by 0.16 standard deviations and reduced stunting by 20% at age
121 18mo⁵¹. We found that mother-infant FUT2 and FUT3 phenotype, where the mother was FUT2+/FUT3-
122 but the infant was not, was associated with greater IYCF reduction of stunting at 18mo. Greater impact
123 of IYCF on stunting was also associated with infant microbiome species maturation, characterized by a
124 shift away from *Bifidobacterium longum* carriage. *B. longum*-dominant microbiome composition was
125 characterized by *B. longum* strains that were most similar to subspecies *infantis*, a proficient HMO
126 utilizer. In addition, *B. longum* abundance and odds of detecting different *B. longum* strains were
127 explained by infant age and differences between mother-infant pairs in FUT2+/FUT3- phenotype.

128

129

130

131

132 **Results**

133 *Mother-infant FUT2+/FUT3- phenotype discordance modifies the effect of IYCF on stunting at 18mo*

134 In a substudy of the SHINE trial, we assessed FUT2 and FUT3 status in mothers and infants from
135 saliva samples. To determine the impact of maternal and infant HBGA on IYCF efficacy, we investigated
136 whether concordance in secretor (FUT2) and Lewis (FUT3) phenotypes between mother and infant pairs
137 modified the effect of IYCF on stunting or LAZ at 18mo. We defined these paired mother-infant
138 phenotypes using combinations of FUT2 and FUT3 status (as presented in Table S1) to more precisely
139 reflect the potential for joint activity of these enzymes in HBGA production (as presented in Figure S1).
140 Each of these paired mother-infant FUT2/FUT3 phenotypes were classified as *both* (if mother and infant
141 shared the same phenotype), *none* (if neither had the phenotype), *infant only* (if the infant had the
142 phenotype but the mother did not) or *mother only* (if the infant did not have the phenotype but the
143 mother did). We fitted multivariable regression models that included terms for the interaction of IYCF
144 and each paired FUT2/FUT3 phenotype between mother and infant, as well as prespecified covariates
145 from the 6mo follow-up visit when IYCF was started, with stunting status at the 18mo visit as the
146 dependent variable. We fitted separate models for each combination of paired mother-infant
147 FUT2/FUT3 phenotype presented in Table S1 and Figure S1. These models were restricted to 792 infants
148 who had both maternal and infant FUT2 and FUT3 status ascertained (Figure S2). Analyses were
149 repeated with LAZ at the 18mo visit as the dependent variable.

150 Amongst infants who were randomized to IYCF, those who were in the *mother only* FUT2+/FUT3-
151 group (13.5%) had a probability of stunting at 18mo that was -33.0% lower (95%CI:-55.0%,-10.0%) than
152 infants in the *both* FUT2+/FUT3- group (11.1%) (Table 1). The *infant only* (11.1%) and *none* (64.3%)
153 FUT2+/FUT3- groups, and other mother-infant FUT2 and FUT3 phenotype combinations (Table S1,
154 Figure S1), did not show evidence of effect modification of IYCF on stunting (Table S2), and there was no
155 evidence of effect modification on LAZ at 18mo after FDR-adjustment for multiple testing (Table S3).

156 Overall, our results indicate that discordance between mothers and infants in the FUT2+/FUT3-
157 phenotype, whereby mothers had the phenotype and infants didn't have the phenotype, was associated
158 with increased efficacy of IYCF to reduce stunting but not to increase LAZ.

159

160 *Infant gut microbiome composition modifies the effect of the IYCF intervention on stunting at 18mo*

161 Given our finding that infants whose mothers were FUT2+/FUT3-, while the infant was not, had
162 greater reductions in stunting by IYCF; and considering the potential importance of FUT2/FUT3
163 phenotypes on early infant microbiome composition via variation in maternal HMO composition and
164 infant gut epithelial HBGA expression, we investigated whether infant gut microbiota species maturation
165 showed evidence for modification of IYCF efficacy on stunting or LAZ at 18mo. First, we used 354 infant
166 metagenomes from 172 infants collected from 1-18mo of age to fit a constrained Principal Coordinates
167 Analysis (PCoA) model that included infant age at stool collection and three dummy variables for
168 mother-infant FUT2+/FUT3- status representing the *none*, *infant only*, and *mother only* groups with the
169 *both* group as the referent (see next section for details). Thus, we derived four PCoA axis scores from
170 this model representing variation in microbiome composition due to infant age and explained by *none*,
171 *infant only*, or *mother only* FUT2+/FUT3- status compared to *both*. Next, we fitted a multivariable
172 regression model that included an IYCF-by-PCoA axis 1 score interaction term and prespecified
173 covariates. The regression model was restricted to 53 infants who had a fecal specimen collected at the
174 6mo follow-up visit when IYCF started and used their covariate values at the 6mo visit (Figure S2).
175 Stunting status at 18mo was used as the dependent variable. We repeated our analyses using PCoA axis
176 2 to 4 scores. Finally, we fitted regression models replacing stunting status with LAZ at 18mo as the
177 dependent variable.

178 Greater PCoA axis 1 scores represented species turnover with increasing infant age (Figure S3), thus
179 reflecting microbiota maturation, while greater PCoA axis 2 scores represented changes in species

180 composition associated with mother-infant FUT2+/FUT3- phenotypes (Figure S3). PCoA axis 1 and 2
181 scores showed evidence of interaction with IYCF on stunting at 18mo (Table 2), but not LAZ (Table S4).
182 Amongst infants randomized to IYCF, those with higher PCoA axis 1 scores at age 6mo were less likely to
183 be stunted at 18mo compared to infants with lower PCoA axis 1 scores (difference-in-differences -76.0%
184 [95%CI: -99.0%,-32.0%, adjusted p=0.003) (Table 2). In contrast, infants randomized to IYCF with higher
185 PCoA axis 2 scores at age 6mo were more likely to be stunted at 18mo compared to infants who had
186 lower PCoA axis 2 scores (difference-in-differences, 14.0% [95%CI: 7.0%,21.0%], adjusted p=0.001)
187 (Table 2). Taken together, our findings showed that infant age-related microbiome species maturation
188 was associated with greater reduction in the probability of stunting at 18mo by IYCF, indicating greater
189 efficacy of the intervention; while microbiome species composition related to mother-infant
190 FUT2+/FUT3- phenotype was associated with lesser reduction in stunting, suggesting variation in
191 microbiome composition due to these infant characteristics is an important determinant of SQ-LNS
192 efficacy to reduce stunting.

193

194 *Infant age and mother-infant FUT2+/FUT3- phenotype explain shifts in microbiome species composition,*
195 *in particular, Bifidobacterium longum*

196 To investigate sources of variation in infant intestinal microbiome composition and derive
197 interpretable measures of species turnover, we performed constrained PCoA of Bray-Curtis
198 dissimilarities with permutational analysis of variance using distance matrices for hypothesis testing.
199 Infant age at stool collection explained 12.6% (ADONIS2 p=0.001) of the variability in microbiome
200 composition (Table S5). Notably, exclusive breastfeeding (EBF) at 3mo was not significantly associated
201 ($R^2=0.346$, ADONIS2 p=0.483) with microbiome composition (Table S5). However, 93.2% of mothers in
202 these analyses reported exclusive breastfeeding (Table S6). Thus, there may not have been sufficient
203 variability in infant breastfeeding practices in this cohort to identify EBF-associated differences between

204 infant microbiomes. Also, inclusion of specimens collected throughout the follow-up period in our PCoA
205 models may have obscured associations with EBF, since EBF is only recommended up to age 6mo.

206 We then fitted a fully adjusted multivariable constrained PCoA model that included both infant age
207 at stool collection and mother-infant FUT2+/FUT3- phenotype. We retained the latter variable to
208 capture variation in microbiota composition associated with mother-infant FUT2+/FUT3- status after
209 controlling for infant age, because of our *a priori* aim to investigate whether microbiome variation due
210 to mother and infant FUT2/FUT3 phenotype was a modifier of the IYCF intervention, and our finding
211 that the *mother only* FUT2+/FUT3- group was associated with a modified intervention effect. In the full
212 model, age explained 12.8% (ADONIS p=0.001) and mother-infant FUT2+/FUT3- phenotype explained
213 0.81% (ADONIS p=0.323) of the variation in microbiome composition (Table S5), indicating that infant
214 age was the main driver of microbiome-wide changes in species composition in this cohort.

215 Age-related maturation in species composition were characterized by decreased relative abundance
216 of *B. longum*, and increased relative abundance of *Prevotella copri*, *Faecalibacterium prausnitzii*, *Dorea*
217 *longicatena*, and *Dorea formicigenerans* (Figure S4). Mother-infant FUT2+/FUT3- discordance was
218 characterized by increased relative abundance of *B. longum* in the *none* and *infant only* groups (Figure
219 S5-S7).

220 In combination with our IYCF-by-PCoA effect modification models (see previous section), these
221 findings indicate that infant microbiota species maturation characterized by a shift away from a
222 microbiome dominated by *B. longum* (i.e. greater PCoA axis 1 score) was associated with a reduction in
223 the probability of stunting at age 18mo in infants randomized to IYCF (Table 2). In contrast, species
224 composition associated with mother-infant FUT2+/FUT3- phenotype (i.e. greater PCoA axis 2 score),
225 which was characterized by higher *B. longum* abundance, showed evidence of reduced impact of IYCF on
226 stunting (Table 2).

227

228 *Bifidobacterium longum* relative abundance modifies the effect of the IYCF intervention on stunting at
229 18mo

230 To determine if differences in the relative abundances of specific microbiome species that
231 characterized the constrained PCoA axes were also associated with significant modification of IYCF on
232 stunting or LAZ at 18mo, we fitted multivariable regression models that included IYCF-by-species relative
233 abundance interaction terms and prespecified covariates as described in the previous sections. These
234 models were restricted to 53 infants who had a fecal specimen collected at the 6mo follow-up visit
235 when IYCF started and used their covariate values at that visit (Figure S2). We fitted a separate model
236 for each microbiome species of interest, defined as those strongly associated with PCoA axis 1 to 4
237 scores (i.e. loadings > 0.5 or < -0.5). Infants randomized to IYCF who had greater relative abundance of
238 *B. longum* when the intervention started were more likely to be stunted at age 18mo compared to
239 infants with lower relative abundance of *B. longum* (differences-in-differences 50.0% [95%CI:
240 26.0%,74.0%], adjusted $p < 0.001$) (Table 3). No other species-level interactions with IYCF on stunting
241 were identified (Table 3). Infants randomized to IYCF with greater *B. longum* relative abundance also
242 had smaller LAZ at 18mo compared to infants with lower *B. longum* abundance; however, this
243 association was not statistically significant after FDR-adjustment (differences-in-differences -0.88[95%CI:
244 -1.45,-0.31], adjusted $p = 0.074$) (Table S7). Overall, our findings indicate that greater relative abundance
245 of *B. longum* in the infant gut microbiome at initiation of the IYCF intervention was associated with less
246 efficacy of the IYCF intervention to reduce stunting at age 18mo.

247

248 *Infants randomized to IYCF in the mother only FUT2+/FUT3- group or with lower B. longum relative*
249 *abundance were spared from more severe growth faltering*

250 To investigate whether these reductions in IYCF efficacy were due to differences in the degree or
251 timing of growth faltering, we plotted (i) LAZ growth trajectories and (ii) LAZ velocities (sd/mo) from 6-

252 18mo of age, by both IYCF arm and paired mother-infant FUT2+/FUT3- phenotype. Infants randomized
253 to IYCF in the *mother only* group had a less steep decline in LAZ trajectories on average compared to
254 infants in the *mother only* group randomized to no IYCF (Figure 1). In addition, although all groups of
255 infants had negative 6-18mo LAZ velocities on average, infants in the *mother only* group who were
256 randomized to IYCF had higher LAZ velocity (-0.02 sd/mo, 95%CI[-0.05,0.00]) compared to those in the
257 no IYCF group (-0.08 sd/mo, 95%CI[-0.11,-0.05]) (Figure 1). Importantly, infants in the *mother only* group
258 also benefitted more from the IYCF intervention in our interaction models (Table 1).

259 We repeated these exploratory analyses to compare LAZ trajectories and LAZ velocities by both IYCF
260 arm and *B. longum* at the 6mo visit stratified above or below the relative abundance median. Infants
261 randomized to IYCF who were above the median relative abundance of *B. longum* had declining growth
262 trajectories on average, while infants below the median did not (Figure 2). Furthermore, the mean 6-
263 18mo LAZ velocity was negative in both *B. longum* groups, but trended toward being higher in the group
264 with relative abundance below (-0.02 sd/mo, 95%CI[-0.07,0.03]) compared to above (-0.08 sd/mo
265 95%CI[-0.12,-0.03]) the median; however, the 95% confidence intervals overlapped. In contrast, among
266 infants randomized to no IYCF, both those with a relative abundance above and those with a relative
267 abundance below the median at the 6mo visit had declining growth trajectories (Figure 2) with similar
268 average negative LAZ velocities (Figure 2).

269 Overall, these results indicate that the differences in IYCF efficacy by mother-infant FUT2+/FUT3-
270 phenotype and *B. longum* relative abundance can be explained by differences in LAZ velocity. Infants in
271 the *mother only* FUT2+/FUT3- group and infants with lower *B. longum* relative abundance at 6mo were
272 spared from more severe LAZ declines, which contributed to a lower probability of stunting at 18mo,
273 even when the differences in velocity were not statistically significant.

274

275 *Bifidobacterium longum* strains most similar to subspecies *infantis* dominate the early infant gut
276 microbiome

277 Next, we aimed to identify whether infants carried different strains of *B. longum* using a pangenome
278 approach. We used PanPhlan3.0⁵² to generate UniProt gene family profiles of dominant *B. longum*
279 strains from 218 infant gut metagenomes, generated from 136 infant, with sufficient coverage of *B.*
280 *longum* (Figure S2). To assess similarities between SHINE *B. longum* strains and previously characterized
281 subspecies, we also included UniProt gene family profiles produced by PanPhlan for 118 reference
282 strains. We performed PCoA using Jaccard dissimilarities calculated from these gene family presence or
283 absence profiles. Three clusters of *B. longum* strains were identifiable by visualization of ordination plots
284 (Figure 3 and S8). We, therefore, performed hierarchical clustering of these Jaccard dissimilarities to
285 delineate three distinct strain clusters and place each strain into the most appropriate cluster (Figure
286 S8). Subspecies *infantis* reference strains predominantly grouped with the largest cluster (hereafter
287 called the *infantis* cluster) and included 15 *infantis* reference strains and 255 SHINE strains (Figure 3).
288 Subspecies *longum* reference strains predominantly grouped with the second largest cluster (*longum*
289 cluster), including 29 *longum*, 3 *infantis*, 64 *unclassified* subspecies strains and 14 SHINE strains. The
290 remaining cluster included two subspecies *suis*, one subspecies *longum*, 4 *unclassified* subspecies
291 reference strains and 15 SHINE strains (*suis* cluster) (Figure 3 and Figure S8).

292

293 *Infant gut microbiome maturation undergoes a transition in which Bifidobacterium longum* strains most
294 *similar to subspecies infantis* become less prevalent

295 To investigate predictors of *B. longum* relative abundance in infants over time, we fitted a
296 longitudinal multivariable zero-inflated mixed-effects model, using 225 specimens from 87 infants with
297 prespecified covariate data. Covariates included infant age at specimen collection, sex, EBF at 3mo,
298 minimum infant dietary diversity at specimen collection, and mother-infant FUT2+/FUT3- phenotypes

299 (Figure S2). Infant age and mother-infant FUT2+/FUT3- phenotype were significant predictors of *B.*
300 *longum* relative abundance. Each one month increase in infant age was associated with a 0.91-fold
301 decrease (95%CI:0.90,0.92, $p < 0.001$) in *B. longum*, and the *mother only* FUT2+/FUT3- group had the
302 lowest relative abundance of *B. longum* throughout follow-up (Figure S11) with a 0.71-fold decrease in
303 relative abundance (95%CI:0.59,0.87, $p = 0.001$) relative to the *both* group (Table S9).

304 Also, to determine predictors of *B. longum* strain cluster detection in infants over time, we fitted
305 multivariable longitudinal logistic regression models using 133 specimens from 70 infants with
306 PanPhlan3.0 output and prespecified covariate data (Figure S2). We fitted a separate model for each
307 strain to estimate its probability of detection. Results were consistent with predictors of *B. longum*
308 relative abundance. Each one month increase in infant age was associated with a 0.85-fold decreased
309 odds (95%CI:0.75,0.96, $p = 0.008$) of the *infantis* cluster (Table S10). At the same time, the *suis* and
310 *longum* clusters increased with age (Table S10 & Figure S12). Female infants had 8.35-fold increased
311 odds of the *infantis* cluster (95%CI:3.17,21.97, $p < 0.001$); and the *infant only* FUT2+/FUT3- group, which
312 had the highest probability of the *infantis* cluster throughout follow-up (Figure S13A), had a 4.66-fold
313 increased odds (95%CI:1.05,20.71, $p = 0.043$) of the *infantis* cluster (Table S10). In contrast, the *mother*
314 *only* FUT2+/FUT3- group had low probability of carrying an *infantis* cluster strain (Figure S13A & Table
315 S10) and the highest probability of carrying a *suis* cluster strain (Figure S13C).

316 In summary, *B. longum* decreased with infant age and was lowest among infants in the *mother only*
317 FUT2+/FUT3- group. The *infantis* cluster, which included the dominant *B. longum* strains, also decreased
318 with infant age. Furthermore, *infantis* cluster strains were most likely to be detected in the *infant only*
319 group, and were less likely to be detected in the *mother only* group, among whom *suis* cluster strains
320 were more likely to be detected. Infant age and mother-infant FUT2+/FUT3- phenotype were important
321 determinants of both *B. longum* relative abundance and strain carriage.

322

323 *Bifidobacterium longum* strains most similar to subspecies *infantis* were characterized by greater
324 capacity for HMO degradation, uptake, siderophore and antimicrobial biosynthesis

325 To identify differences in metabolic potential between *B. longum* strain clusters, we used two-sided
326 Fisher's Exact tests to compare UniProt gene family presence between clusters. We restricted these
327 analyses to the 284 SHINE *Bifidobacterium* pangenomes to make inferences about differences in
328 metabolic potential between SHINE strains. We then performed overrepresentation analyses⁵³ of
329 differentially frequent gene families by one-sided Fisher's Exact test to determine whether they were
330 more likely to be involved in specific GO biological processes⁵⁴, or to function as specific carbohydrate-
331 active enzymes (CAZymes)⁵⁵ or transporters⁵⁶. Gene families that were more common in the *infantis*
332 cluster were more likely to be involved in HMO degradation, and included genes that function as
333 CAZyme Glycoside Hydrolase Family 20 (GH20) (β -N-acetylglucosaminidases, β -N-
334 acetylgalactosaminidase, β -6-SO₃-N-acetylglucosaminidases, and lacto-N-biosidases), GH29
335 (fucosidases), GH95 (fucosidases), and GH33 (sialidases) (Figure 4A, Table S8). Conversely, gene families
336 that were more common in the other clusters were more likely to be involved in degradation of plant-
337 derived polysaccharides, including genes that function as GH42 (β -galactosidases), GH51 (L-
338 arabinofuranosidases) and GH127 (β -L-arabinofuranosidase) CAZymes (Figure 4A, Table S8). Similarly,
339 gene families that were more common in the *infantis* cluster were more likely to function as
340 transporters involved in oligosaccharide uptake (TCID 3.A.1.1.59), while those that were less common in
341 the *infantis* cluster were more likely to be involved in uptake of fructose and other sugars (TCID
342 3.A.1.2.23) (Figure 4A, Table S8). Other differences between strain clusters included greater carriage of
343 gene families among *infantis* cluster strains that are involved in riboflavin biosynthesis, signal
344 transduction, amino acid catabolism and uptake.

345 We also identified differences between strain clusters in the frequency of 115 MetaCyc⁵⁷ pathways
346 identified using MinPath⁵⁸ (Figure S10). Pathways that were more common in the *infantis* cluster were

347 more likely to be involved in generation of precursor metabolites and energy, and secondary metabolite
348 biosynthesis (which predominantly included pathways for biosynthesis of siderophores and
349 antimicrobials) (Figure 4B, Table S8). Conversely, the *infantis* cluster was less likely to include pathways
350 involved in glycan metabolism and polymeric compound degradation (e.g. pectin, xylan, and
351 arabinogalactan degradation pathways), and in fatty acid and lipid biosynthesis (Figure 4B, Table S8).

352 Overall, infant gut microbiomes were dominated by *B. longum* strains that were most similar to
353 subspecies *infantis* in their UniProt gene family profiles. The primary distinction of *B. longum* strains in
354 the *infantis* cluster was greater capacity for HMO degradation and uptake of oligosaccharides than
355 plant-derived polysaccharides. However, strains in the *infantis* cluster also had greater capacity for
356 siderophore and antimicrobial production, and displayed differences in their capacity for riboflavin, fatty
357 acid, and lipid metabolism.

358

359 **Discussion**

360 In this study of HIV-unexposed infants enrolled in the SHINE trial in rural Zimbabwe, we tested the
361 hypothesis that mother-infant FUT2/FUT3 phenotype and infant gut microbiome modify the effect of an
362 intervention containing small-quantity lipid based nutrient supplements, on infant stunting and LAZ at
363 18mo of age. Our goal was to define mechanisms that explain the rather modest effects of SQ-LNS on
364 linear growth, reasoning that maternal-infant HBGA phenotypes might be important given their
365 combined role in shaping the early-life microbiome. We found the following features are associated with
366 greater reduction in stunting at 18mo by IYCF: (i) discordance in mother-infant FUT2+/FUT3- phenotype,
367 where the mother has the phenotype but the infant does not; (ii) changes in microbiome species
368 composition that reflected a shift from a *B. longum*-dominant microbiome to a microbiome with less *B.*
369 *longum* and a greater abundance of species characteristic of older infants; and (iii) decreased *B. longum*
370 abundance that was associated with paired mother-infant FUT+/FUT3- status. These findings suggest

371 that a persistently “younger” microbiome, characterized by a high abundance of *B. longum* and carriage
372 of *B. longum* strains best suited to HMO metabolism, at the point when complementary foods are
373 introduced into the infant diet, may modify the effects of an intervention that includes SQ-LNS on infant
374 stunting.

375 The *mother only* FUT2+/FUT3- group showed evidence of a greater reduction in stunting following
376 receipt of one year of the IYCF intervention. Mother-infant FUT2+/FUT3- phenotype was also a
377 significant predictor of *B. longum*, whereby relative abundance was lower throughout follow-up in the
378 *mother only* group. Active maternal FUT2/FUT3 genes are key determinants of milk oligosaccharide
379 composition³¹⁻³³. Human milk specimens form distinct groups based on maternal FUT2⁵⁹ and FUT3
380 phenotype^{31,33} by principal component analyses of oligosaccharide composition. In particular,
381 FUT2+/FUT3- mothers are a subset of FUT2+ women who form an HMO cluster that is distinct from
382 mothers with other phenotypes, including FUT2+ mothers who are also FUT3+^{31,33}. Differences in HMO
383 composition influence growth and activity of Bifidobacterium populations in the infant gut^{28,59}. Host
384 FUT2 status may also affect infant gut microbiome composition³⁶⁻⁴⁰. Gut Bifidobacterium³⁹,
385 Bacteroides^{36,38}, Faecalibacterium⁴⁰ and Roseburia⁴⁰ are differentially abundant in FUT2+ compared to
386 FUT2- individuals. However, reported differences in microbiome composition by FUT2/FUT3 status have
387 been inconsistent, potentially due to variability in age, dietary patterns, host health, sampled gut
388 sections and methodology between studies^{60,614}, and studies predominantly included adults. However,
389 CAZymes found in *B. longum* species that function in HMO degradation (GH29 and GH95) have also been
390 found to function in host intestinal glycan degradation in infants⁶². The evidence, therefore, suggests
391 that the FUT2/FUT3 phenotypes of mother and infant, together, can elicit a strong prebiotic selective
392 pressure, driven by maternal milk and infant glycan composition²⁸ that influences Bifidobacteria and
393 broader gut microbiota composition in infants.

394 In contrast to our finding that mother-infant FUT2+/FUT3- phenotype predicted the presence of *B.*
395 *longum* subspecies *infantis* cluster strains, a prior study reported that maternal or infant FUT2 or FUT3
396 status did not predict the abundance of subspecies *infantis* or *longum* in children⁶³. However, we
397 included infant age as a covariate in our models, while the prior study did not⁶³. In addition, to
398 accommodate the fact that FUT2 and FUT3 work in concert biologically to produce different HBGAs and
399 HMOs (Figure S1), we defined combined FUT2 and FUT3 phenotypes. Another smaller study found
400 infants born to FUT2+/FUT3- mothers had lower bifidobacterial operational taxonomic unit diversity
401 compared to other infants³⁹. This study provides additional evidence that maternal FUT2+/FUT3-
402 phenotype is associated with bifidobacterial taxon composition in the infant gut. Furthermore, we
403 considered paired maternal and infant phenotypes⁶³. More research is needed to clarify the roles of
404 mother-infant FUT2/FUT3, maternal HMOs and the infant glyco biome as drivers of infant gut
405 microbiome composition and development.

406 In our PCoA model, infant microbiome species maturation predominantly reflected decreased
407 abundance of *B. longum* and increased abundance of *P. copri*, *F. prausnitzii*, *D. longicatena*, and *D.*
408 *formicigenerans*. These species were also important predictors of infant age in a microbiome-age model
409 previously developed from this same cohort⁶⁴. Age-discriminatory taxa in the same genera were also
410 identified in previously reported microbiome-age models¹⁴. Delayed gut microbiota-age has been
411 reported in children with severe acute malnutrition (SAM), while improvements in microbiota-age and
412 relative abundance of age-discriminatory taxa have been correlated with better growth¹⁴. Our analyses
413 complement this literature with evidence that infant gut microbiome species maturation increased the
414 effect of the IYCF intervention on stunting at 18mo, while greater relative abundance of *B. longum*, an
415 age-discriminatory taxon which is associated with younger age, reduced the effect. This suggests that
416 delayed maturation of the gut microbiome at the point when complementary foods are introduced and
417 IYCF is initiated, may impair IYCF-induced effects on growth.

418 Infant age was the strongest determinant of *B. longum* relative abundance over time. This is
419 consistent with previous reports⁶⁵. In breastfed infants, Bifidobacteria are the most abundant gut
420 bacteria^{65,66}. Human breast milk is rich in oligosaccharides, which Bifidobacteria preferentially utilize⁶⁷.
421 At introduction of solid foods, a wider variety of nutrients and reduced availability of HMOs correspond
422 to a decrease in Bifidobacterium,⁶⁸ greater bacterial diversity and evenness, and development of a more
423 adult-like composition by 2–3 years of age^{11,69–71}.

424 Utilization of HMOs by Bifidobacterium varies between species and strains^{72–78}. We identified three
425 clusters of dominant *B. longum* strains that also varied by infant age and mother-infant FUT2+/FUT3-
426 phenotype. The cluster of strains with pangenomes most closely resembling subspecies *infantis* had the
427 highest prevalence in early infancy. However, by age 18mo there was a marked decrease in detection of
428 *infantis* cluster strains and a corresponding increase in detection of strains with pangenomes most
429 similar to subspecies *suis*, which had the highest prevalence at 18mo. Strains most similar to subspecies
430 *longum* increased more slowly. This finding is consistent with a recent study that also reported a pattern
431 of succession among three distinct gut *B. longum* clades from birth to 24mo of age. Subspecies *infantis*
432 was dominant in early infancy but peaked at age 6mo and decreased considerably thereafter. While a
433 transitional clade that included strains most similar to subspecies *suis* and *suillum* showed a
434 corresponding increase in abundance that peaked by 18mo, and subspecies *longum* expanded from
435 15mo-24mo of age⁷⁹. In that report, the transitional *suis/suillum* clade harbored functional capacity to
436 degrade both HMOs and dietary polysaccharides, suggesting it may be an adaptation of the infant gut
437 microbiome to a period when breastfeeding may co-occur with introduction of complementary foods⁷⁹.
438 We add to this work by showing that differences between mother and infant in FUT2+/FUT3- phenotype
439 may also play a role in driving this transition, whereby, throughout follow-up, the *mother only*
440 FUT2+/FUT3- group had a low prevalence of the *infantis* cluster and the highest prevalence of the *suis*
441 cluster; while the *infantis* cluster was most prevalent in the *infant only* group.

442 *B. longum* subspecies *infantis* are particularly well adapted for HMO utilization^{80,81}. *B. longum*
443 subspecies *longum*, on the other hand, do not grow as well on HMO, and are more specialized for
444 utilization of diet-derived polysaccharides⁸². In our analyses, UniProt gene families that were more
445 frequent in the *infantis* cluster were more likely to be involved in HMO degradation and uptake. Two of
446 CAZyme families more likely to be carried by the *infantis* cluster (GH29⁸³ and GH33⁷⁴) were previously
447 reported as more prevalent in subspecies *infantis* strains. In contrast, UniProt gene families that were
448 less frequent in the *infantis* cluster were more likely to be involved in uptake of fructose and other
449 simple sugars, including the sugar transporter 3.A.1.2.23, which was previously described in a different
450 *B. longum* subspecies⁸⁴. Furthermore, strains in the *suvis* and *longum* clusters were more likely to carry
451 UniProt gene families involved in such MetaCyc pathways as pectin, xylan, and arabinogalactan
452 degradation. UniProt gene families found more frequently in *infantis* cluster strains were also more
453 likely to be involved in siderophore and antimicrobial biosynthesis. Heavy metals such as iron and zinc
454 are essential minerals for nearly all bacteria and their mammalian hosts. Strategies utilized by bacteria
455 to acquire heavy metals include siderophore biosynthesis. Siderophores are low molecular weight iron-
456 chelating compounds that are synthesized by bacteria to scavenge iron and other essential metals such
457 as zinc under nutrient-restricted conditions⁸⁵. For example, Bifidobacterium species isolated from iron-
458 deficient children efficiently sequester iron via siderophore production⁸⁶. Siderophores may provide a
459 competitive advantage to Bifidobacteria⁸⁷, which along with antimicrobial biosynthesis⁸⁸, may also help
460 protect the infant gut from enteric pathogens that require essential metals for colonization. However,
461 essential metals such as iron and zinc are key components in SQ-LNS formulations⁸⁹⁻⁹¹, and produce
462 improvements in linear growth and reductions in stunting risk^{92,936}. While siderophore activity varies
463 considerably between Bifidobacterium species and strains, no research to date has investigated
464 sequestration of essential metals by subspecies *infantis* strains commonly found in resource-limited
465 settings. Overall, our analyses suggest that greater abundance of *B. longum*, at the time when IYCF is

466 started, characterized by a predominance of strains with carriage of gene families which confer greater
467 capacity for HMO utilization and siderophore biosynthesis, is associated with lower impact to reduce
468 stunting at 18mo. These suggest potential mechanisms by which a “younger” microbiome may constrain
469 the beneficial effects of an SQ-LNS intervention on infant stunting. However, more research is required
470 to fully elucidate the biological mechanisms and downstream pathways to stunting that could be
471 involved.

472 Our results are in contrast to a previous RCT that investigated infant microbiome composition as a
473 modifier of SQ-LNS impact on infant growth in Malawi⁴⁸. However, in the primary analyses of that RCT,
474 there was no effect of SQ-LNS on linear infant growth⁹⁴. Furthermore, SQ-LNS was provided to both
475 mothers during pregnancy and infants starting at 6mo postpartum, active control interventions (iron-
476 folate or multiple micronutrient supplements) were provided to mothers^{48,94}, and 16S rRNA gene
477 amplification and sequencing were used to characterize the microbiota which can affect both taxon
478 detection (including *Bifidobacterium*) and study results⁹⁵. A second RCT reported evidence for effect
479 modification of iron supplementation on growth by maternal FUT2 status, where infants of FUT2-
480 mothers randomized to iron supplementation showed greater declines in LAZ than infants of FUT2+
481 mothers⁹⁶. In addition, a third, recent RCT found that suppression of *B. longum* by amoxicillin allowed
482 the gut microbiota of children with SAM to better adapt to a solid-food diet by reducing the abundance
483 of taxa specialized for breast milk utilization, resulting in improved anthropometric indicators of infant
484 nutritional status⁹⁷. However, it is essential to note that *B. longum* subspecies *infantis* is a critical early
485 infant gut bacteria with important benefits for infant health, including protection from enteric
486 pathogens⁹⁸, immune system development⁹⁹, and reducing asthma risk¹⁰⁰. *B. longum* subspecies *infantis*
487 also improved ponderal growth when administered to infants ~4mo of age with SAM in two RCTs^{101,102}.
488 However, the effects on LAZ were not statistically significant. Our work complements this literature. Our
489 findings suggest that a shift away from a “less mature” microbiome, characterized by a high abundance

490 of *B. longum* and carriage of strains that are better suited to HMO metabolism, may be critical to
491 support efficacy of nutrient supplements that start with the introduction of complementary feeding; and
492 we identify maternal drivers of early infant *B. longum* abundance and strain carriage which, if further
493 elucidated, may be employed to shape the infant microbiome into a more favorable composition at this
494 critical time in infancy.

495 There are some limitations of this work. First, from our cohort of 1169 HIV-unexposed infants, we
496 had microbiome data on 172 infants. However, infants included in our analyses were comparable to
497 infants who excluded (Table S6). Also, mother-infant FUT2+/FUT3- phenotype, which was an important
498 determinant of *B. longum* abundance and strain cluster detection, modified the impact of IYCF on
499 stunting in the larger sample of 792 infants without measured microbiome data in a way that was
500 consistent with our microbiome results. That said, our small sample size may have limited power to
501 detect effect modification by other taxa that are indicative of a “more mature” post-weaning
502 microbiome. Our analyses were not able to investigate effect modification by actual microbial metabolic
503 activity, maternal HMO composition or infant gut glyco biome, which would require multi-omics
504 approaches such as metatranscriptomics and metabolomics. Finally, it is possible that the delay in
505 microbiome maturation we characterized may reflect some reverse causality, where sick or non-thriving
506 children are put to the breast more with higher relative breastmilk intake. However, this behavior would
507 need to systematically occur less often in the subset of mothers and their infants who were discordant
508 for FUT2+/FUT3- that we describe to fully explain our results, thus we think this explanation is unlikely.

509 In conclusion, we present analyses of moderators of IYCF impact on infant stunting at 18mo in an
510 RCT of IYCF using SQ-LNS in rural Zimbabwe. We report that (i) infant microbiome species maturation,
511 characterized by a shift from *B. longum* dominance, particularly *B. longum* strains that are most similar
512 to the proficient HMO utilizer subspecies *infantis*, was associated with increased IYCF reduction of
513 stunting risk at age 18mo; (ii) discordance in mother-infant FUT2+/FUT3- phenotype, where the mother

514 had the phenotype but the infant did not, was associated with increased IYCF reduction of stunting risk;
515 and (iii) reduction in *B. longum* relative abundance was also determined by mother-infant FUT2+/FUT3-
516 phenotype. Future work should investigate how differences between maternal HMOs and infant gut
517 glycans determine gut Bifidobacterium species and strain composition, and investigate how to tailor
518 interventions at the introduction of complementary feeding to balance infant nutritional needs with
519 age-related microbiome composition and function to prevent stunting.

520

521 **Figure legends**

522 **Figure 1. Infant growth trajectories and growth velocities vary by IYCF arm and mother-infant** 523 **FUT2+/FUT3- phenotype.**

524 (A) LAZ by infant age from 1-18mo (n=792), stratified by IYCF arm (light grey, no IYCF; dark grey, IYCF)
525 and mother-infant FUT2+/FUT3- phenotype (*both, none, infant only or mother only*). Lines illustrate
526 average trajectories. Shaded areas are 95% confidence bands. Infants randomized to IYCF in the *mother*
527 *only* group had a less steep decline in LAZ trajectories on average compared to infants randomized to no
528 IYCF.

529 (B) Violin plots of LAZ velocity from 6-18mo of age, stratified by IYCF arm (light grey, no IYCF; dark grey,
530 IYCF) and mother-infant FUT2+/FUT3- phenotype (*both, none, infant only or mother only*). Open circles
531 with error bars in the center of each panel indicate mean LAZ velocity and 95% CIs. All groups of infants
532 had negative LAZ velocities on average, but infants in the *mother only* group who were randomized to
533 IYCF had higher LAZ velocity on average, contributing to a less steep decline in LAZ over time and a
534 smaller proportion of infants stunted at 18mo.

535

536 **Figure 2. Infant growth trajectories and growth velocities vary by IYCF arm and infant gut** 537 ***Bifidobacterium longum* relative abundance.**

538 (A) LAZ by infant age from 1-18mo (n=53), stratified by IYCF arm and *Bifidobacterium longum* relative
539 abundance (light grey, \leq median relative abundance; dark grey, $>$ median relative abundance). Thin lines
540 illustrate individual trajectories. Thick lines show average trajectories. Infants randomized to IYCF who
541 were above the median relative abundance had a declining growth trajectory on average, while infants
542 below the median did not.

543 (B) Violin plots of LAZ velocity from 6-18mo of age, stratified by IYCF arm (light grey, no IYCF; dark grey,
544 IYCF) and mother-infant FUT2+/FUT3- phenotype (*both, none, infant only* or *mother only*). Open circles
545 with error bars indicate mean LAZ velocity and 95% CIs. All groups of infants had negative LAZ velocities
546 on average. However, LAZ velocity trended toward being higher in the group with relative abundance
547 below the median. The 95% confidence intervals overlap, but the higher LAZ velocity contributed to a
548 less steep decline in LAZ over time and a smaller proportion of stunted infants at 18mo.

549

550 **Figure 3. *Bifidobacterium longum* strains most similar to subspecies *infantis* dominate the early infant**
551 **gut microbiome.** Ordination plots of PCoA with Jaccard dissimilarities calculated using the pangenome
552 profiles of dominant *Bifidobacterium longum* strains in fecal specimens (N=284) generated using
553 PanPhlan3.0. Three clusters of *B. longum* strains were identifiable. Individual strains are indicated by
554 small circles. Those in the same cluster are enclosed by a large ellipse and are differentiated by both the
555 color of the ellipse and the border color of the small circle (blue, *infantis*; dark green, *longum*; red, *suis*).
556 Filled small circles indicate reference strains (light blue, *infantis*; pink, *suis*; light green, *longum*; grey,
557 *unclassified*). Open small circles indicate SHINE strains. Subspecies *infantis* reference strains
558 predominantly grouped with the largest cluster (blue ellipse, *infantis* cluster). Subspecies *longum*
559 reference strains predominantly grouped with the second largest cluster (dark green ellipse, *longum*
560 cluster). The remaining cluster (red ellipse, *suis* cluster) grouped with subspecies *suis* and *longum*.

561

562 **Figure 4. SHINE infant *Bifidobacterium longum infantis* cluster strains are better adapted for human**
563 **milk oligosaccharide utilization and protection against pathogens than *suis* and *longum* cluster strains.**

564 (A) Heatmap of UniProt gene family presence in SHINE infant *Bifidobacterium longum* strains (N=284).
565 UniProt gene family presence is indicated in grey. The horizontal bar at the top indicates strain cluster
566 (blue, *infantis*; dark green, *longum*; red, *suis*). Vertical bars from left to right indicate: UniProt gene
567 families that differed in prevalence between the *infantis* and *longum* cluster by two-sided Fisher's Exact
568 test after FDR correction (red); UniProt gene families that differed in prevalence between the *infantis*
569 and *suis* cluster by two-sided Fisher's Exact test after FDR correction (red); Biological Process GO groups;
570 CAZymes; and Transporter class. Only gene families with evidence of overrepresentation in a Biological
571 Process, CAZyme or Transporter class by one-sided Fisher's Exact Test are presented.

572 (B) Heatmap of MetaCyc pathway presence in SHINE infant *Bifidobacterium longum* strains (N=284).
573 MetaCyc pathway presence is indicated in grey. The horizontal bar at the top indicates strain cluster
574 (blue, *infantis*; dark green, *longum*; red, *suis*). Vertical bars from left to right indicate: MetaCyc pathways
575 that differed in prevalence between the *infantis* and *longum* cluster by two-sided Fisher's Exact test
576 after FDR correction (red); MetaCyc pathways that differed in prevalence between the *infantis* and *suis*
577 cluster by two-sided Fisher's Exact test after FDR correction (red); MetaCyc pathway type. Only
578 pathways with evidence of overrepresentation in a pathway type by one-sided Fisher's Exact Test are
579 presented.

580

581 **Methods**

582 *Study design and participants*

583 The Sanitation Hygiene Infant Nutrition Efficacy (SHINE) trial was a 2x2 factorial cluster-randomized
584 trial that enrolled 5280 pregnant women at a median age of 12.5 weeks gestation between November
585 2012 and March 2015 to test the impact of improved household water quality, sanitation, and hygiene

586 (WASH) and improved infant and young child feeding (IYCF) via provision of SQ-LNS to the infant from
587 age 6mo-18mo, on linear growth and anemia at age 18mo. A detailed description of the SHINE trial
588 design and methods has been published^{51,103}.

589 Briefly, research nurses made home visits twice during pregnancy and at infant ages 1, 3, 6, 12, and
590 18 months. At baseline, maternal education and age, household wealth¹⁰⁴, existing water and sanitation
591 services, and household food security¹⁰⁵ were assessed, and mothers were tested for HIV via a rapid
592 testing algorithm. Infant birth date, weight, and delivery details were transcribed from health facility
593 records. Gestational age at delivery was calculated from the date of the mother's last menstrual period
594 ascertained at baseline. Infant weight, length, and mid-upper arm circumference were measured at
595 every postnatal visit. Nurses were standardized against a gold-standard anthropometrist every 6
596 months, with retraining provided to those who failed to meet predefined criteria.

597 Part-way through the trial (from mid-2014 onwards) mother-infant pairs were invited to join a
598 substudy to collect additional biological specimens. Women were informed about the substudy at their
599 32-week gestation visit and those with live births were enrolled at the 1-month postnatal visit, or as
600 soon as possible thereafter^{106,107}.

601

602 *Specimen collection and processing*

603 Mothers collected fecal specimens prior to the research nurse visit. Fecal specimens were placed in
604 a cold box and transported to the field laboratory, where they were stored at -80°C until transfer to the
605 central laboratory in Harare for long-term archiving at -80°C, with generator back-up. Fecal specimens
606 were transferred via private courier on dry ice from Harare, Zimbabwe to Vancouver, British Columbia
607 for metagenomic analyses.

608 The Qiagen DNeasy PowerSoil Kit was used to extract total DNA from 200mg of feces, according to
609 manufacturer's instructions. Paired-end libraries were constructed using the Illumina TruSeq kit and

610 using New England Biosystem TruSeq compatible library preparation reagents. Libraries were sequenced
611 at the British Columbia Genome Sciences Centre using the Illumina HiSeq 2500 platform. Forty-eight
612 libraries were pooled and included per sequencing lane. Negative controls were included to capture
613 microbial contamination in the DNA extraction and library preparation steps.

614 The analyses presented here utilize data and specimens from HIV-uninfected mothers and their
615 infants enrolled in the specimen collection substudy. The fecal microbiome was characterized in 354
616 specimens collected from 172 HIV-unexposed infants from 1 to 18mo of age. A mean(sd) of 2.0(1.0)
617 samples were analyzed per child. Infants included in these analyses largely resembled the population of
618 live-born infants from the wider SHINE trial who were not included in these analyses (Table S6).
619 However, infants in the current analyses had slightly older mothers and longer gestational ages, and
620 fewer were born during the hungry season, but more were in a household that met the minimum
621 dietary diversity score (Table S6). Overall, the majority were born by vaginal delivery (91.6%) in an
622 institution (91.5%) and were exclusively breastfed (83.2% at 3 months). The prevalence of stunting was
623 26.9% at 18mo in this sub-study (Table S6).

624

625 *Bioinformatics*

626 Sequenced reads were trimmed of adapters and filtered to remove low-quality, short (<60 base-
627 pairs), and duplicate reads, as well as those of human, other animal or plant origin using KneadData with
628 default settings. Overall, 354 unique whole metagenome sequencing datasets were used from fecal
629 specimens collected from 1mo to 18mo from 172 infants with available mother and infant FUT2 and
630 FUT3 phenotypes (Figure S2). On average, 10.8 ± 3.7 million paired end quality-filtered reads were
631 generated per sample. Assessment of negative controls and technical variation have been previously
632 reported⁶⁴. Species composition was determined by mapping reads to clade-specific markers using
633 MetaPhlAn3, while functional gene and metabolic pathway composition was determined using

634 HUMAnN3 against the UniRef90 database, both with default settings⁵². Bacterial species and pathway
635 abundance estimates were normalized to relative abundances. UniProt gene family profiles were
636 generated for dominant *B. longum* strains in fecal metagenomes with sufficient coverage for
637 pangenome analysis using PanPhlan3⁵². To facilitate interpretation of UniProt gene family profiles, the
638 minimum set of biological pathways sufficient to explain the gene families identified in each strain was
639 determined using MinPath with default settings⁵⁸ and the MetaCyc database⁵⁷.

640

641 *Assessment of FUT2 and FUT3 status*

642 Saliva samples were collected by oral swab from mothers and infants. Available saliva from any
643 follow-up visit was selected to assess FUT2 and FUT3 status. Secretor versus non-secretor (FUT2) and
644 Lewis-positive versus Lewis-null (FUT3) status were ascertained for infants and their mothers using a
645 previously reported phenotyping assay¹⁰⁸. We defined FUT2 and FUT3 phenotype combinations as
646 Lewis-positive non-secretors (FUT2-/FUT3+), Lewis-positive secretors (FUT+/FUT3+), or Lewis-null
647 secretors (FUT2+/FUT3-) (Table S11) according to the histo-blood group antigen synthesis pathways
648 defined in Figure S1. Paired mother-infant phenotype concordance or discordance was defined as
649 presented in Table S1.

650 Of 1,169 mother-infant pairs, 999 (85.4%) mothers and 1104 (94.4%) infants were tested. Of these,
651 FUT2 or FUT3 status could be determined in 889 (76.0%) and 999 (85.4%) mothers and infants,
652 respectively (Table S11). Of those whose FUT2 or FUT3 status could be ascertained, secretors were the
653 most frequent FUT2 phenotype (88.1% and 85.6% in mothers and infants respectively), while Lewis-
654 positive was the most frequent FUT3 phenotype (76.8% and 74.9% in mothers and infants, respectively)
655 (Table S11). Most mothers and infants were Lewis-positive secretors (60.5% and 64.9%, respectively),
656 followed by FUT2+/FUT3- (25.1% and 23.2%, respectively), and Lewis-positive non-secretors (14.4% and
657 11.9%, respectively) (Table S1).

658

659 *Statistical analyses*

660 Infant characteristics that explain species β -diversity were evaluated using constrained principal
661 coordinates analysis (PCoA) of Bray-Curtis dissimilarities (*capscale*)¹⁰⁹. Characteristics of interest
662 included factors that are known to be correlated with microbiome composition (infant age, sex, EBF at
663 3mo, dietary diversity, maternal and infant FUT2 and FUT3 phenotype). Statistical significance was
664 tested by permutational analysis of variance using distance matrices with 1000 permutations
665 (*adonis2*)¹¹⁰. We then developed a final multivariable constrained PCoA model that included covariates
666 which explained a significant fraction ($p < 0.05$) of the variance in microbiome composition (infant age at
667 specimen collection), as well as mother-infant FUT2+/FUT3- discordance given our *a priori* hypothesis
668 that FUT2 and FUT3 phenotypes are important determinants of infant microbiome composition and our
669 finding that mother-infant FUT2+/FUT3- discordance was an important modifier of IYCF efficacy to
670 reduce stunting at 18mo. Constrained PCoA axis scores in the final multivariable model represented
671 changes in microbiome composition (species turnover) along gradients defined by each infant
672 characteristic included in the full model.

673 Since the IYCF intervention was started at the 6mo follow-up visit, we assessed interaction between
674 randomization to IYCF and mother-infant FUT2+/FUT3- discordance or microbiome composition using
675 data from the 6mo visit as covariates. The primary outcome was stunting at 18mo and LAZ at 18mo was
676 a secondary outcome. We fitted separate models for stunting and LAZ at 18mo. Interaction was
677 assessed on the additive risk difference scale, which is most appropriate for statistical estimation of
678 synergistic biological effects¹¹¹. We used generalized linear models (*glm*) with a Gaussian distribution, an
679 identity link, sandwich standard errors (*sandwich*)¹¹² and an IYCF-by-mother-infant FUT2+/FUT3-
680 phenotype interaction term. We repeated these analyses using IYCF-by-PCoA axis score interaction
681 terms, where PCoA axis scores were derived from the final multivariable constrained PCoA model. One

682 model was fitted per constrained PCoA axis. For species that were strongly associated with PCoA axis
683 scores (loadings > 0.5 or < -0.5), analyses were repeated to assess IYCF-by-species interactions. We fitted
684 a separate model for each species of interest. Models also included IYCF, infant sex, mother-infant
685 FUT2+/FUT3- discordance, infant age at specimen collection, an indicator of whether infants met the
686 minimum dietary diversity score at specimen collection, and LAZ at specimen collection. We did not
687 include WASH arm because, in prior analyses, the SHINE WASH intervention did not affect stunting or
688 LAZ at 18mo⁵¹ nor infant gut microbiome composition⁶⁴. P-values were adjusted for multiple hypothesis
689 testing to preserve the false discovery rate¹¹³.

690

691 *Identification and analysis of Bifidobacterium longum strain clusters*

692 *B. longum* strain profiles produced with PanPhlan3.0, which indicate whether UniProt gene families
693 are present in a strain¹¹⁴, were converted to Jaccard dissimilarity matrices and visualized by PCoA to
694 ascertain the existence of strain clusters (*capscale*). Three clusters were identified, and strain cluster
695 membership was determined by hierarchical clustering of Jaccard dissimilarities and Ward's error sum of
696 squares algorithm (*hclust*)¹¹⁵. Hierarchical clustering dendrograms were cut at a height to obtain three
697 clusters.

698 Differences in UniProt gene family profiles between *B. longum* strain clusters were determined by
699 two-sided Fisher's Exact test (*fisher.test*), with adjustment for multiple hypothesis testing to preserve
700 the false discovery rate¹¹³, and were visualized using heatmaps (*heatmap3*). 3260 UniProt gene families
701 were differentially present between strain clusters after FDR-adjustment. We performed
702 overrepresentation analyses⁵³ using one-sided Fisher's Exact tests (*fisher.test*) to determine whether the
703 differentially present gene families were more likely to function as particular CAZymes⁵⁵ or
704 transporters⁵⁶, or in specific GO biological processes⁵⁴. These analyses were repeated using the
705 biological pathways determined with MinPath⁵⁸. 115 pathways were differentially present between

706 strain clusters after FDR-adjustment. We performed overrepresentation analyses of these pathways to
707 determine whether they were more likely to have particular biological functions defined by MetaCyc
708 pathway types.

709

710 *Predictors of Bifidobacterium relative abundance and strain detection*

711 Predictors of *B. longum* relative abundance over time were assessed using mixed-effects zero-
712 inflated beta regression estimated by restricted maximum likelihood (*gamlss*)¹¹⁶. The model included
713 infant age at specimen collection, sex, EBF at 3mo, minimum infant dietary diversity at specimen
714 collection, and mother-infant FUT2+/FUT3- discordance, with random intercepts (*re*) and a first order
715 autocorrelation structure (*corCAR1*).

716 Predictors of *B. longum* strain cluster were assessed by logistic regression (*glm*) using an indicator of
717 strain cluster presence as the dependent variable, with the same covariates, and sandwich standard
718 errors. An individual model was fitted separately for each cluster. Bias corrected¹¹⁷ logistic regression
719 was used to facilitate stable parameter estimation due to separation resulting from the small sample
720 size¹¹⁸.

721 All statistical analyses were conducted in R version 4.2.0. PCoA and adonis2 were performed using
722 the *vegan* package¹¹⁹. Heatmaps were generated with *heatmap3*. Mixed-effects zero-inflated beta
723 regression was performed using the *gamlss* package¹²⁰. Bias corrected logistic regression models were
724 fitted using the *brglm2* package. Sandwich standard errors were generated with the *sandwich* package.

725

726 *Resource availability*

727 **Lead contact**

728 Further information and requests for resources and reagents should be directed to and will be fulfilled
729 by the lead contact, Ethan Gough (egough1@jh.edu).

730 **Materials availability**

731 This study did not generate new unique reagents.

732 **Data and code availability**

733 The raw metagenome sequencing data generated in this study have been deposited in the European
734 Bioinformatics Database under accession code PRJEB51728. Final processed and annotated
735 metagenome sequencing data files (taxa and pathways) are available at

736 <https://doi.org/10.5281/zenodo.7471082>. Epidemiologic data files are available at Code for statistical
737 analyses are available from the corresponding author upon request.

738

739 **Supplemental Tables**

740 **Table S8. Overrepresentation of UniProt gene families and Metacyc pathways, which differ between**
741 **strain clusters, by GO biological process, CAZyme or Transporter class or Metacyc pathway type.**

742

743 **Ethics approvals**

744 All SHINE mothers provided written informed consent. The Medical Research Council of Zimbabwe
745 (MRCZ/A/1675), Johns Hopkins Bloomberg School of Public Health (JHU IRB # 4205.), and the University
746 of British Columbia Ethics Board (H15-03074) approved the study protocol, including the microbiome
747 analyses. The SHINE trial is registered at ClinicalTrials.gov (NCT01824940).

748

749 **Acknowledgments**

750 We thank all the mothers, babies, and their families who participated in the SHINE trial and all members
751 of the SHINE trial team (all members listed here: <https://doi.org/10.1093/cid/civ844>). We particularly
752 thank the leadership and staff of the Ministry of Health and Child Care in Chirumanzu and Shurugwi
753 districts and Midlands Province (especially environmental health, nursing, and nutrition) for their roles

754 in operationalization of the study procedures, the Ministry of Local Government officials in each district
755 who supported and facilitated field operations, Phillipa Rambanepasi and her team for proficient
756 management of all the finances, Virginia Sauramba for management of compliance issues, and the
757 programme officers at the Bill & Melinda Gates Foundation and the Department for International
758 Development (UK Aid), who enthusiastically worked with us over a long period to make SHINE happen.

759 Funding was from the Bill & Melinda Gates Foundation (OPP1021542 and OPP1143707; J.H.H. and
760 A.J.P.), with a subcontract to the University of British Columbia (20R25498; A.R.M.). United Kingdom
761 Department for International Development (DFID/UKAID; J.H.H. and A.J.P.). Wellcome Trust
762 (093768/Z/10/Z, 108065/Z/15/Z, 206455/Z/17/Z, 203905/Z/16/Z and 210807/Z/18/Z; A.J.P., R.C.R. and
763 C.E.). Swiss Agency for Development and Cooperation (J.H.H. and A.J.P.). US National Institutes of Health
764 (2R01HD060338-06; J.H.H.). UNICEF (PCA-2017-0002; J.H.H. and A.J.P.). The Nutricia Research
765 Foundation (2021-52; E.K.G.) The funders had no role in the design of the study and collection, analysis,
766 and interpretation of data and in writing the manuscript.

767

768 **Author contributions:** A.R.M., L.E.S., R.J.S., M.N.N.M., J.H.H. and A.J.P. conceptualized and designed the
769 study. K.M., R.N., B.C., F.D.M., N.V.T., J.T., and B.M. collected data and biospecimens. H.M.G., I.B.,
770 S.K.G., R.C.R., F.F. and L.C. processed fecal specimens. M.K. conducted laboratory analyses to ascertain
771 FUT2 and FUT3 status. C.E., J.C. and E.K.G. developed the FUT2 and FUT3 analysis plan. E.K.G. developed
772 and conducted the microbiome statistical analysis plan. T.J.E. and E.K.G. conducted bioinformatics.
773 A.R.M. and E.K.G. analyzed and interpreted the data. E.K.G. wrote the original manuscript draft. All
774 authors reviewed the manuscript. A.R.M., A.J.P. and J.H.H. supervised and verified the data.

775

776 **Declaration of interests:** T.J.E. was paid a scientific consulting fee in relation to the analysis of the data
777 presented here by the Zvitambo Institute for Maternal and Child Health Research. All other authors
778 declare no competing interests.

779

780

781

782

783

784

785

786

787

788

789

790

791

792

793

794

Table 1. Multivariable regression model¹ to estimate modification of IYCF on stunting at 18mo by mother-infant Lewis-null secretor phenotype discordance among 792 infants in whom mother and infant FUT2 and FUT3 status was ascertained

| | <u>Main Effect</u> | | | <u>Difference-in-Differences for IYCF by FUT2 and FUT3 phenotype combination</u> | | |
|-------------------------|--------------------|---------|-------------------------------|--|---------|-------------------------------|
| | PD (95%CI) | p-value | Adjusted p-value ² | PD (95%CI) | p-value | Adjusted p-value ² |
| Both FUT2+/FUT3- | ref | ref | ref | ref | ref | |
| None FUT2+/FUT3- | 0.13(0.01,0.25) | 0.041 | 0.330 | -0.21(-0.42,-0.01) | 0.039 | 0.118 |
| Infant only FUT2+/FUT3- | 0.15(-0.03,0.33) | 0.094 | 0.277 | -0.21(-0.48,0.06) | 0.127 | 0.191 |
| Mom only FUT2+/FUT3- | 0.29(0.14,0.44) | 0.000 | 0.007 | -0.33(-0.55,-0.10) | 0.005 | 0.015 |
| non-IYCF | ref | ref | ref | | | |
| IYCF | 0.16(-0.02,0.35) | 0.138 | 0.177 | | | |

¹Covariates include season of birth, birthweight, infant sex, ever exclusive breastfeeding at 3mo, age at the 6mo visit, infant WHZ at the 6mo visit, and infant LAZ at the 6mo visit

²Adjusted for multiple hypothesis testing by the Benjamini-Hochberg method

PD, prevalence difference; 95%CI, 95% confidence interval; ref, referent

796

797

798

799

800

801

802

803

804

805

806

807

808

809

810
811
812
813
814

Table 2. Multivariable regression models¹ to estimate modification of IYCF on stunting at 18mo by infant gut microbiome species turnover in 53 infants

| | PD(95%CI) | p-value | Adjusted p-value ² |
|--------------------------------|--------------------|------------------|-------------------------------|
| PCoA Axis 1 | | <u>n/N=17/53</u> | |
| IYCF | -0.51(-0.99,-0.12) | 0.009 | 0.045 |
| PC1 | 0.21(-0.99,0.45) | 0.085 | 0.204 |
| PC1-by-IYCF³ | -0.76(-0.99,-0.32) | 0.001 | 0.003 |
| PCoA Axis 2 | | <u>n/N=17/53</u> | |
| IYCF | -0.14(-0.99,0.12) | 0.293 | 0.469 |
| PC2 | -0.06(-0.99,-0.01) | 0.020 | 0.068 |
| PC2-by-IYCF³ | 0.14(0.07,0.21) | <0.001 | 0.001 |
| PCoA Axis 3 | | <u>n/N=17/53</u> | |
| IYCF | 0.09(-0.99,0.39) | 0.543 | 0.686 |
| PC3 | 0.04(-0.99,0.09) | 0.156 | 0.340 |
| PC3-by-IYCF³ | -0.08(-0.99,-0.02) | 0.016 | 0.032 |
| PCoA Axis 4 | | <u>n/N=17/53</u> | |
| IYCF | 0.03(-0.99,0.31) | 0.847 | 0.924 |
| PC4 | 0.00(-0.99,0.06) | 0.994 | 0.994 |
| PC4-by-IYCF³ | 0.03(-0.99,0.12) | 0.438 | 0.501 |

¹Covariates include birthweight, infant sex, age at the 6mo visit, infant LAZ at the 6mo visit, infant diet diversity score at the 6mo visit, and mother-infant Lewis-null secretor phenotype discordance coded as both, none, infant only or mother only

²Adjusted for multiple hypothesis testing by the Benjamini-Hochberg method

³Differences-in-differences

PD, prevalence difference; 95%CI, 95% confidence interval

815
816
817
818
819

820

821

Table 3. Multivariable regression models¹ to estimate modification of IYCF on stunting at 18mo by infant gut microbiome species in 53 infants

| | PD(95%CI) | p-value | Adjusted p-value ² |
|--|--------------------|------------------|-------------------------------|
| Bifidobacterium longum | | <u>n/N=17/53</u> | |
| IYCF | -0.16(-0.43,0.10) | 0.232 | 0.976 |
| B.longum | -0.24(-0.43,-0.05) | 0.014 | 0.068 |
| B.longum-by-IYCF ³ | 0.50(0.26,0.74) | <0.001 | <0.001 |
| Bifidobacterium pseudocatenulatum | | <u>n/N=17/53</u> | |
| IYCF | -0.54(-1.02,-0.06) | 0.029 | 0.304 |
| B.pseudocatenulatum | 1.82(0.48,3.15) | 0.008 | 0.051 |
| B.pseudocatenulatum-by-IYCF ³ | -2.00(-3.33,-0.68) | 0.003 | 0.014 |
| Escherichia coli | | <u>n/N=17/53</u> | |
| IYCF | 0.04(-0.25,0.33) | 0.774 | 1.000 |
| E.coli | 0.01(-0.10,0.13) | 0.823 | 0.859 |
| E.coli-by-IYCF ³ | -0.07(-0.21,0.08) | 0.362 | 0.592 |
| Dorea longicatena | | <u>n/N=17/53</u> | |
| IYCF | 0.02(-0.27,0.31) | 0.896 | 1.000 |
| D.longicatena | -0.02(-0.13,0.09) | 0.725 | 0.859 |
| D.longicatena-by-IYCF ³ | 0.03(-0.39,0.44) | 0.898 | 0.898 |
| Dorea formicigenerans | | <u>n/N=17/53</u> | |
| IYCF | -0.18(-0.37,0.01) | 0.062 | 0.324 |
| D.formicigenerans | -0.18(-0.33,-0.03) | 0.018 | 0.073 |
| D.formicigenerans-by-IYCF ³ | -0.50(-1.00,-0.00) | 0.048 | 0.145 |

¹Covariates include birthweight, infant sex, age at the 6mo visit, infant LAZ at the 6mo visit, infant diet diversity score at the 6mo visit, and mother-infant Lewis-null secretor phenotype discordance coded as both, none, infant only or mother only

²Adjusted for multiple hypothesis testing by the Benjamini-Hochberg method

³Differences-in-differences

PD, prevalence difference; 95%CI, 95% confidence interval

822

823

824

825

826

827

828 **References**

- 829 1. United Nations Children’s Fund, World Health Organization, and The World Bank (2019). Levels
830 and trends in child malnutrition: key findings of the 2019 Edition of the Joint Child Malnutrition
831 Estimates – UNICEF Regions. (United Nations Children’s Fund (UNICEF), World Health Organization,
832 International Bank for Reconstruction and Development/The World Bank).
- 833 2. Onis, M.D., Garza, C., Onyango, A.W., and Martorell, R. (2006). WHO child growth standards. *Acta*
834 *Paediatrica* 95, 1–104.
- 835 3. Benjamin-Chung, J., Mertens, A., Colford, J.M., Hubbard, A.E., van der Laan, M.J., Coyle, J.,
836 Sofrygin, O., Cai, W., Nguyen, A., Pokpongkiat, N.N., et al. (2023). Early-childhood linear growth
837 faltering in low- and middle-income countries. *Nature* 621, 550–557.
- 838 4. Gough, E.K., Moodie, E.E.M., Prendergast, A.J., Ntozini, R., Moulton, L.H., Humphrey, J.H., Manges,
839 A.R., Stephens, D.A., Moodie, E.E.M., Prendergast, A.J., et al. (2016). Linear growth trajectories in
840 Zimbabwean infants. *American Journal of Clinical Nutrition* 104, 1616–1627.
- 841 5. Adair, L.S.L.S., Fall, C.H.D.D., Osmond, C., Stein, A.D.A.A.D., Martorell, R., Ramirez-Zea, M.,
842 Sachdev, H.S., Dahly, D.L., Bas, I., Norris, S.A., et al. (2013). Associations of linear growth and
843 relative weight gain during early life with adult health and human capital in countries of low and
844 middle income: Findings from five birth cohort studies. *The Lancet* 382, 525–534.
- 845 6. Victora, C.G., Adair, L., Fall, C., Hallal, P.C., Martorell, R., Richter, L., and Sachdev, H.S. (2008).
846 Maternal and child undernutrition: consequences for adult health and human capital. *Lancet* 371,
847 340–357.
- 848 7. Vollmer, S., Harttgen, K., Subramanyam, M.A., Finlay, J., Klasen, S., and Subramanian, S.V. (2014).
849 Association between economic growth and early childhood undernutrition: evidence from 121
850 Demographic and Health Surveys from 36 low-income and middle-income countries. *The Lancet*
851 *Global Health* 2, e225-234.
- 852 8. Dewey, K.G., Wessells, K.R., Arnold, C.D., Prado, E.L., Abbeddou, S., Adu-Afarwuah, S., Ali, H.,
853 Arnold, B.F., Ashorn, P., Ashorn, U., et al. (2021). Characteristics that modify the effect of small-
854 quantity lipid-based nutrient supplementation on child growth: an individual participant data
855 meta-analysis of randomized controlled trials. *Am J Clin Nutr* 114, 15S-42S.
- 856 9. Dewey, K.G., Arnold, C.D., Wessells, K.R., Prado, E.L., Abbeddou, S., Adu-Afarwuah, S., Ali, H.,
857 Arnold, B.F., Ashorn, P., Ashorn, U., et al. (2022). Preventive small-quantity lipid-based nutrient
858 supplements reduce severe wasting and severe stunting among young children: an individual
859 participant data meta-analysis of randomized controlled trials. *Am J Clin Nutr* 116, 1314–1333.

- 860 10. Ruel, M.T., Alderman, H., and Maternal Child Nutrition Study Group (2013). Nutrition-sensitive
861 interventions and programmes: how can they help to accelerate progress in improving maternal
862 and child nutrition? *Lancet* 382, 536–551.
- 863 11. Arrieta, M.-C., Stiemsma, L.T., Amenyogbe, N., Brown, E.M., and Finlay, B. (2014). The intestinal
864 microbiome in early life: health and disease. *Frontiers in Immunology* 5, 427.
- 865 12. Jones, H.J., Bourke, C.D., Swann, J.R., and Robertson, R.C. (2023). Malnourished Microbes: Host–
866 Microbiome Interactions in Child Undernutrition. *Annual Review of Nutrition* 43, 327–353.
- 867 13. Robertson, R.C., Manges, A.R., Finlay, B.B., and Prendergast, A.J. (2019). The Human Microbiome
868 and Child Growth - First 1000 Days and Beyond. *Trends Microbiol* 27, 131–147.
- 869 14. Subramanian, S., Huq, S., Yatsunenkov, T., Haque, R., Mahfuz, M., Alam, M.A., Benezra, A.,
870 DeStefano, J., Meier, M.F., Muegge, B.D., et al. (2014). Persistent gut microbiota immaturity in
871 malnourished Bangladeshi children. *Nature* 510, 417–421.
- 872 15. Zhao, G., Vatanen, T., Droit, L., Park, A., Kostic, A.D., Poon, T.W., Vlamakis, H., Siljander, H.,
873 Härkönen, T., Hämäläinen, A.M., et al. (2017). Intestinal virome changes precede autoimmunity in
874 type I diabetes-susceptible children. *Proceedings of the National Academy of Sciences of the*
875 *United States of America* 114, E6166–E6175. 10.1073/pnas.1706359114.
- 876 16. Ho, N.T., Li, F., Lee-Sarwar, K.A., Tun, H.M., Brown, B.P., Pannaraj, P.S., Bender, J.M., Azad, M.B.,
877 Thompson, A.L., Weiss, S.T., et al. (2018). Meta-analysis of effects of exclusive breastfeeding on
878 infant gut microbiota across populations. *Nature Communications* 9, 4169. 10.1038/s41467-018-
879 06473-x.
- 880 17. Reyes, A., Blanton, L.V., Cao, S., Zhao, G., Manary, M., Trehan, I., Smith, M.I., Wang, D., Virgin,
881 H.W., Rohwer, F., et al. (2015). Gut DNA viromes of Malawian twins discordant for severe acute
882 malnutrition. *Proceedings of the National Academy of Sciences of the United States of America*
883 112, 11941–11946. 10.1073/pnas.1514285112.
- 884 18. Gough, E.K., Stephens, D.A., Moodie, E.M., Prendergast, A.J., Stoltzfus, R.J., Humphrey, J.H., and
885 Manges, A.R. (2016). Linear growth faltering in infants is associated with *Acidaminococcus* sp. and
886 community-level changes in the gut microbiota. *Microbiome* 3, 24.
- 887 19. Ghosh, T.S., Gupta, S.S., Bhattacharya, T., Yadav, D., Barik, A., Chowdhury, A., Das, B., Mande, S.S.,
888 and Nair, G.B. (2014). Gut Microbiomes of Indian Children of Varying Nutritional Status. *PLoS ONE*
889 9, e95547.
- 890 20. Gupta, S.S., Mohammed, M.H., Ghosh, T.S., Kanungo, S., Nair, G.B., and Mande, S.S. (2011).
891 Metagenome of the gut of a malnourished child. *Gut Pathog* 3, 7.
- 892 21. Huey, S.L., Jiang, L., Fedarko, M.W., McDonald, D., Martino, C., Ali, F., Russell, D.G., Udipi, S.A.,
893 Thorat, A., Thakker, V., et al. (2020). Nutrition and the Gut Microbiota in 10- to 18-Month-Old
894 Children Living in Urban Slums of Mumbai, India. *mSphere* 5, e00731-20.

- 895 22. Digitale, J., Sié, A., Coulibaly, B., Ouermi, L., Dah, C., Tapsoba, C., Bärnighausen, T., Lebas, E., Arzika,
896 A.M., Glymour, M.M., et al. (2020). Gut Bacterial Diversity and Growth among Preschool Children
897 in Burkina Faso. *Am J Trop Med Hyg* 103, 2568–2573.
- 898 23. Collard, J.-M., Andrianonimiadana, L., Habib, A., Rakotondrainipiana, M., Andriantsalama, P.,
899 Randriamparany, R., Rabenandrasana, M. a. N., Weill, F.-X., Sauvonnet, N., Rendremanana, R.V., et
900 al. (2022). High prevalence of small intestine bacteria overgrowth and asymptomatic carriage of
901 enteric pathogens in stunted children in Antananarivo, Madagascar. *PLoS Negl Trop Dis* 16,
902 e0009849.
- 903 24. Kamng'ona, A.W., Young, R., Arnold, C.D., Kortekangas, E., Patson, N., Jorgensen, J.M., Prado, E.L.,
904 Chaima, D., Malamba, C., Ashorn, U., et al. (2019). The association of gut microbiota characteristics
905 in Malawian infants with growth and inflammation. *Scientific Reports* 9.
- 906 25. Perin, J., Burrowes, V., Almeida, M., Ahmed, S., Haque, R., Parvin, T., Biswas, S., Azmi, I.J., Bhuyian,
907 S.I., Talukder, K.A., et al. (2020). A Retrospective Case-Control Study of the Relationship between
908 the Gut Microbiota, Enteropathy, and Child Growth. *The American journal of tropical medicine and*
909 *hygiene*.
- 910 26. Brown, E.M., Wlodarska, M., Willing, B. p, Vonaesch, P., Han, J., Reynolds, L.A., Arriet, M.-C., Uhrig,
911 M., Scholz, R., Partida, O., et al. (2015). Diet and specific microbial exposure trigger features of
912 environmental enteropathy in a novel murine model. *Nature Communications* 6, 7806.
- 913 27. Kau, A.L., Planer, J.D., Liu, J., Rao, S., Yatsunenkov, T., Trehan, I., Manary, M.J., Liu, T.-C.,
914 Stappenbeck, T.S., Maleta, K.M., et al. (2015). Functional characterization of IgA-targeted bacterial
915 taxa from undernourished Malawian children that produce diet-dependent enteropathy. *Science*
916 *Translational Medicine* 7, 276ra24-276ra24.
- 917 28. Salli, K., Hirvonen, J., Siitonen, J., Ahonen, I., Anglenius, H., and Maukonen, J. (2021). Selective
918 Utilization of the Human Milk Oligosaccharides 2-Fucosyllactose, 3-Fucosyllactose, and
919 Difucosyllactose by Various Probiotic and Pathogenic Bacteria. *Journal of Agricultural and Food*
920 *Chemistry* 69.
- 921 29. Davis, J.C.C., Totten, S.M., Huang, J.O., Nagshbandi, S., Kirmiz, N., Garrido, D.A., Lewis, Z.T., Wu,
922 L.D., Smilowitz, J.T., German, J.B., et al. (2016). Identification of Oligosaccharides in Feces of
923 Breast-fed Infants and Their Correlation with the Gut Microbial Community*. *Molecular & Cellular*
924 *Proteomics* 15, 2987–3002.
- 925 30. Charbonneau, M.R., O'Donnell, D., Blanton, L.V., Totten, S.M., Davis, J.C.C., Barratt, M.J., Cheng, J.,
926 Guruge, J., Talcott, M., Bain, J.R., et al. (2016). Sialylated Milk Oligosaccharides Promote
927 Microbiota-Dependent Growth in Models of Infant Undernutrition. *Cell* 164, 859–871.
- 928 31. Mank, M., Hauner, H., Heck, A.J.R., and Stahl, B. (2020). Targeted LC-ESI-MS2 characterization of
929 human milk oligosaccharide diversity at 6 to 16 weeks post-partum reveals clear staging effects
930 and distinctive milk groups. *Anal Bioanal Chem* 412, 6887–6907.
- 931 32. Castanys-Muñoz, E., Martin, M.J., and Prieto, P.A. (2013). 2'-fucosyllactose: an abundant,
932 genetically determined soluble glycan present in human milk. *Nutr Rev* 71, 773–789.

- 933 33. Blank, D., Dotz, V., Geyer, R., and Kunz, C. (2012). Human milk oligosaccharides and Lewis blood
934 group: individual high-throughput sample profiling to enhance conclusions from functional studies.
935 *Adv Nutr* 3, 440S-9S.
- 936 34. Schneider, M., Al-Shareffi, E., and Haltiwanger, R.S. (2017). Biological functions of fucose in
937 mammals. *Glycobiology* 27, 601–618.
- 938 35. Cooling, L. (2015). Blood groups in infection and host susceptibility. *Clinical Microbiology Reviews*
939 28.
- 940 36. Tong, M., McHardy, I., Ruegger, P., Goudarzi, M., Kashyap, P.C., Haritunians, T., Li, X., Graeber,
941 T.G., Schwager, E., Huttenhower, C., et al. (2014). Reprogramming of gut microbiome energy
942 metabolism by the FUT2 Crohn's disease risk polymorphism. *ISME J* 8, 2193–2206.
- 943 37. Rausch, P., Rehman, A., Künzel, S., Häsler, R., Ott, S.J., Schreiber, S., Rosenstiel, P., Franke, A., and
944 Baines, J.F. (2011). Colonic mucosa-associated microbiota is influenced by an interaction of crohn
945 disease and FUT2 (Secretor) genotype. *Proceedings of the National Academy of Sciences of the*
946 *United States of America* 108.
- 947 38. Gampa, A., Engen, P.A., Shobar, R., and Mutlu, E.A. (2017). Relationships between gastrointestinal
948 microbiota and blood group antigens. *Physiol Genomics* 49, 473–483.
- 949 39. Wacklin, P., Mäkivuokko, H., Alakulppi, N., Nikkilä, J., Tenkanen, H., Råbinä, J., Partanen, J., Aranko,
950 K., and Mättö, J. (2011). Secretor genotype (FUT2 gene) is strongly associated with the
951 composition of bifidobacteria in the human intestine. *PLoS ONE* 6, e20113.
- 952 40. Rühlemann, M.C., Hermes, B.M., Bang, C., Doms, S., Moitinho-Silva, L., Thingholm, L.B., Frost, F.,
953 Degenhardt, F., Wittig, M., Kässens, J., et al. (2021). Genome-wide association study in 8,956
954 German individuals identifies influence of ABO histo-blood groups on gut microbiome. *Nat Genet*
955 53, 147–155.
- 956 41. Christensen, L., Vuholm, S., Roager, H.M., Nielsen, D.S., Krych, L., Kristensen, M., Astrup, A., and
957 Hjorth, M.F. (2019). Prevotella Abundance Predicts Weight Loss Success in Healthy, Overweight
958 Adults Consuming a Whole-Grain Diet Ad Libitum: A Post Hoc Analysis of a 6-Wk Randomized
959 Controlled Trial. *J Nutr* 149, 2174–2181.
- 960 42. Eriksen, A.K., Brunius, C., Mazidi, M., Hellström, P.M., Risérus, U., Iversen, K.N., Fristedt, R., Sun, L.,
961 Huang, Y., Nørskov, N.P., et al. (2020). Effects of whole-grain wheat, rye, and lignan
962 supplementation on cardiometabolic risk factors in men with metabolic syndrome: a randomized
963 crossover trial. *Am J Clin Nutr* 111, 864–876. 10.1093/ajcn/nqaa026.
- 964 43. Shin, J.-H., Jung, S., Kim, S.-A., Kang, M.-S., Kim, M.-S., Joung, H., Hwang, G.-S., and Shin, D.-M.
965 (2019). Differential Effects of Typical Korean Versus American-Style Diets on Gut Microbial
966 Composition and Metabolic Profile in Healthy Overweight Koreans: A Randomized Crossover Trial.
967 *Nutrients* 11, E2450.
- 968 44. Hjorth, M.F., Roager, H.M., Larsen, T.M., Poulsen, S.K., Licht, T.R., Bahl, M.I., Zohar, Y., and Astrup,
969 A. (2018). Pre-treatment microbial Prevotella-to-Bacteroides ratio, determines body fat loss
970 success during a 6-month randomized controlled diet intervention. *Int J Obes (Lond)* 42, 580–583.

- 971 45. Li, Y., Wang, D.D., Satija, A., Ivey, K.L., Li, J., Wilkinson, J.E., Li, R., Baden, M., Chan, A.T.,
972 Huttenhower, C., et al. (2021). Plant-Based Diet Index and Metabolic Risk in Men: Exploring the
973 Role of the Gut Microbiome. *J Nutr* *151*, 2780–2789.
- 974 46. Li, J., Li, Y., Ivey, K.L., Wang, D.D., Wilkinson, J.E., Franke, A., Lee, K.H., Chan, A., Huttenhower, C.,
975 Hu, F.B., et al. (2022). Interplay between diet and gut microbiome, and circulating concentrations
976 of trimethylamine N-oxide: findings from a longitudinal cohort of US men. *Gut* *71*, 724–733.
- 977 47. Wang, D.D., Nguyen, L.H., Li, Y., Yan, Y., Ma, W., Rinott, E., Ivey, K.L., Shai, I., Willett, W.C., Hu, F.B.,
978 et al. (2021). The gut microbiome modulates the protective association between a Mediterranean
979 diet and cardiometabolic disease risk. *Nat Med* *27*, 333–343.
- 980 48. Hughes, R.L., Arnold, C.D., Young, R.R., Ashorn, P., Maleta, K., Fan, Y.-M., Ashorn, U., Chaima, D.,
981 Malamba-Banda, C., Kable, M.E., et al. (2020). Infant gut microbiota characteristics generally do
982 not modify effects of lipid-based nutrient supplementation on growth or inflammation: secondary
983 analysis of a randomized controlled trial in Malawi. *Sci Rep* *10*, 14861.
- 984 49. Smith, M.I., Yatsunenko, T., Manary, M.J., Trehan, I., Mkakosya, R., Cheng, J., Kau, A.L., Rich, S.S.,
985 Concannon, P., Mychaleckyj, J.C., et al. (2013). Gut microbiomes of Malawian twin pairs discordant
986 for Kwashiorkor. *Science* *339*, 548–554.
- 987 50. Schwarzer, M., Makki, K., Storelli, G., Machuca-Gayet, I., Srutkova, D., Hermanova, P., Martino,
988 M.E., Balmand, S., Hudcovic, T., Heddi, A., et al. (2016). *Lactobacillus plantarum* strain maintains
989 growth of infant mice during chronic undernutrition. *Science* *351*, 854–857.
- 990 51. Humphrey, J.H., Mbuya, M.N.N., Ntozini, R., Moulton, L.H., Stoltzfus, R.J., Tavengwa, N.V., Mutasa,
991 K., Majo, F.D., Mutasa, B., Mangwadu, G., et al. (2019). Independent and combined effects of
992 improved water, sanitation, and hygiene, and improved complementary feeding, on child stunting
993 and anaemia in rural Zimbabwe: a cluster-randomised trial. *The Lancet Global Health* *7*, e132–
994 e147.
- 995 52. Beghini, F., McIver, L.J., Blanco-Míguez, A., Dubois, L., Asnicar, F., Maharjan, S., Mailyan, A.,
996 Manghi, P., Scholz, M., Thomas, A.M., et al. (2021). Integrating taxonomic, functional, and strain-
997 level profiling of diverse microbial communities with bioBakery 3. *Elife* *10*, e65088.
- 998 53. Wieder, C., Frainay, C., Poupin, N., Rodriguez-Mier, P., Vinson, F., Cooke, J., Lai, R.P., Bundy, J.G.,
999 Jourdan, F., and Ebbels, T. (2021). Pathway analysis in metabolomics: Recommendations for the
1000 use of over-representation analysis. *PLoS Comput Biol* *17*, e1009105.
- 1001 54. The Gene Ontology Consortium, Aleksander, S.A., Balhoff, J., Carbon, S., Cherry, J.M., Drabkin, H.J.,
1002 Ebert, D., Feuermann, M., Gaudet, P., Harris, N.L., et al. (2023). The Gene Ontology knowledgebase
1003 in 2023. *Genetics* *224*, iyad031.
- 1004 55. Drula, E., Garron, M.-L., Dogan, S., Lombard, V., Henrissat, B., and Terrapon, N. (2022). The
1005 carbohydrate-active enzyme database: functions and literature. *Nucleic Acids Res* *50*, D571–D577.
- 1006 56. Saier, M.H., Reddy, V.S., Moreno-Hagelsieb, G., Hendargo, K.J., Zhang, Y., Iddamsetty, V., Lam,
1007 K.J.K., Tian, N., Russum, S., Wang, J., et al. (2021). The Transporter Classification Database (TCDB):
1008 2021 update. *Nucleic Acids Res* *49*, D461–D467.

- 1009 57. Caspi, R., Billington, R., Fulcher, C.A., Keseler, I.M., Kothari, A., Krummenacker, M., Latendresse,
1010 M., Midford, P.E., Ong, Q., Ong, W.K., et al. (2018). The MetaCyc database of metabolic pathways
1011 and enzymes. *Nucleic Acids Research* *46*, D633–D639.
- 1012 58. Ye, Y., and Doak, T.G. (2009). A parsimony approach to biological pathway
1013 reconstruction/inference for genomes and metagenomes. *PLoS Comput Biol* *5*, e1000465.
- 1014 59. Bazanella, M., Maier, T.V., Clavel, T., Lagkouvardos, I., Lucio, M., Maldonado-Gómez, M.X., Autran,
1015 C., Walter, J., Bode, L., Schmitt-Kopplin, P., et al. (2017). Randomized controlled trial on the impact
1016 of early-life intervention with bifidobacteria on the healthy infant fecal microbiota and
1017 metabolome. *American Journal of Clinical Nutrition* *106*, 1274–1286.
- 1018 60. Davenport, E.R., Cusanovich, D.A., Michelini, K., Barreiro, L.B., Ober, C., and Gilad, Y. (2015).
1019 Genome-wide association studies of the human gut microbiota. *PLoS ONE* *10*.
1020 10.1371/journal.pone.0140301.
- 1021 61. Turpin, W., Bedrani, L., Espin-Garcia, O., Xu, W., Silverberg, M.S., Smith, M.I., Guttman, D.S.,
1022 Griffiths, A., Moayyedi, P., Panaccione, R., et al. (2018). FUT2 genotype and secretory status are
1023 not associated with fecal microbial composition and inferred function in healthy subjects. *Gut*
1024 *Microbes* *9*.
- 1025 62. Bell, A., and Juge, N. (2021). Mucosal glycan degradation of the host by the gut microbiota.
1026 *Glycobiology* *31*, 691–696.
- 1027 63. Colston, J.M., Taniuchi, M., Ahmed, T., Ferdousi, T., Kabir, F., Mduma, E., Nshama, R., Iqbal, N.T.,
1028 Haque, R., Ahmed, T., et al. (2022). Intestinal Colonization With *Bifidobacterium longum*
1029 Subspecies Is Associated With Length at Birth, Exclusive Breastfeeding, and Decreased Risk of
1030 Enteric Virus Infections, but Not With Histo-Blood Group Antigens, Oral Vaccine Response or Later
1031 Growth in Three Birth Cohorts. *Front Pediatr* *10*, 804798.
- 1032 64. Robertson, R.C., Edens, T.J., Carr, L., Mutasa, K., Gough, E.K., Evans, C., Geum, H.M., Baharmand, I.,
1033 Gill, S.K., Ntozini, R., et al. (2023). The gut microbiome and early-life growth in a population with
1034 high prevalence of stunting. *Nat Commun* *14*, 654.
- 1035 65. Stewart, C.J., Ajami, N.J., O'Brien, J.L., Hutchinson, D.S., Smith, D.P., Wong, M.C., Ross, M.C., Lloyd,
1036 R.E., Doddapaneni, H.V., Metcalf, G.A., et al. (2018). Temporal development of the gut microbiome
1037 in early childhood from the TEDDY study. *Nature* *562*, 583–588.
- 1038 66. Yatsunenko, T., Rey, F.E., Manary, M.J., Trehan, I., Dominguez-Bello, M.G., Contreras, M., Magris,
1039 M., Hidalgo, G., Baldassano, R.N., Anokhin, A.P., et al. (2012). Human gut microbiome viewed
1040 across age and geography. *Nature* *486*, 222–228.
- 1041 67. Marcobal, A., and Sonnenburg, J.L. (2012). Human milk oligosaccharide consumption by intestinal
1042 microbiota: Human milk oligosaccharide consumption. *Clinical Microbiology and Infection* *18*, 12–
1043 15.
- 1044 68. Bäckhed, F., Roswall, J., Peng, Y., Feng, Q., Jia, H., Kovatcheva-Datchary, P., Li, Y., Xia, Y., Xie, H.,
1045 Zhong, H., et al. (2015). Dynamics and stabilization of the human gut microbiome during the first
1046 year of life. *Cell Host and Microbe* *17*, 690–703. 10.1016/j.chom.2015.04.004.

- 1047 69. Collado, M.C., Cernada, M., Bäuerl, C., Vento, M., and Pérez-Martínez, G. (2012). Microbial ecology
1048 and host-microbiota interactions during early life stages. *Gut Microbes* 3, 352–365.
- 1049 70. Matamoros, S., Gras-Leguen, C., Vacon, F.L., Potel, G., and Cochetiere, M.-F. de L. (2013).
1050 Development of intestinal microbiota in infants and its impact on health. *Trends in Microbiology*
1051 21, 167–173.
- 1052 71. Laursen, M.F. (2021). Gut Microbiota Development: Influence of Diet from Infancy to Toddlerhood.
1053 *Annals of Nutrition and Metabolism*.
- 1054 72. Lewis, Z.T., Totten, S.M., Smilowitz, J.T., Popovic, M., Parker, E., Lemay, D.G., Van Tassell, M.L.,
1055 Miller, M.J., Jin, Y.-S., German, J.B., et al. (2015). Maternal fucosyltransferase 2 status affects the
1056 gut bifidobacterial communities of breastfed infants. *Microbiome* 3, 13.
- 1057 73. Ojima, M.N., Jiang, L., Arzamasov, A.A., Yoshida, K., Odamaki, T., Xiao, J., Nakajima, A., Kitaoka, M.,
1058 Hirose, J., Urashima, T., et al. (2022). Priority effects shape the structure of infant-type
1059 Bifidobacterium communities on human milk oligosaccharides. *ISME J* 16, 2265–2279.
- 1060 74. Li, M., Zhou, X., Stanton, C., Ross, R.P., Zhao, J., Zhang, H., Yang, B., and Chen, W. (2021).
1061 Comparative Genomics Analyses Reveal the Differences between *B. longum* subsp. *infantis* and *B.*
1062 *longum* subsp. *longum* in Carbohydrate Utilisation, CRISPR-Cas Systems and Bacteriocin Operons.
1063 *Microorganisms* 9, 1713.
- 1064 75. Gotoh, A., Katoh, T., Sakanaka, M., Ling, Y., Yamada, C., Asakuma, S., Urashima, T., Tomabechi, Y.,
1065 Katayama-Ikegami, A., Kurihara, S., et al. (2018). Sharing of human milk oligosaccharides
1066 degradants within bifidobacterial communities in faecal cultures supplemented with
1067 Bifidobacterium bifidum. *Scientific Reports* 8, 13958.
- 1068 76. Sakanaka, M., Gotoh, A., Yoshida, K., Odamaki, T., Koguchi, H., Xiao, J.-Z., Kitaoka, M., and
1069 Katayama, T. (2019). Varied Pathways of Infant Gut-Associated Bifidobacterium to Assimilate
1070 Human Milk Oligosaccharides: Prevalence of the Gene Set and Its Correlation with Bifidobacteria-
1071 Rich Microbiota Formation. *Nutrients* 12, 71. 10.3390/nu12010071.
- 1072 77. Garrido, D., Ruiz-Moyano, S., Lemay, D.G., Sela, D.A., German, J.B., and Mills, D.A. (2015).
1073 Comparative transcriptomics reveals key differences in the response to milk oligosaccharides of
1074 infant gut-associated bifidobacteria. *Sci Rep* 5, 13517.
- 1075 78. Garrido, D., Ruiz-Moyano, S., Kirmiz, N., Davis, J.C., Totten, S.M., Lemay, D.G., Ugalde, J.A.,
1076 German, J.B., Lebrilla, C.B., and Mills, D.A. (2016). A novel gene cluster allows preferential
1077 utilization of fucosylated milk oligosaccharides in Bifidobacterium longum subsp. longum SC596.
1078 *Sci Rep* 6, 35045.
- 1079 79. Vatanen, T., Ang, Q.Y., Siegwald, L., Sarker, S.A., Le Roy, C.I., Duboux, S., Delannoy-Bruno, O.,
1080 Ngom-Bru, C., Boulangé, C.L., Stražar, M., et al. (2022). A distinct clade of Bifidobacterium longum
1081 in the gut of Bangladeshi children thrives during weaning. *Cell* 185, 4280-4297.e12.
- 1082 80. Sela, D.A., Chapman, J., Adeuya, A., Kim, J.H., Chen, F., Whitehead, T.R., Lapidus, A., Rokhsar, D.S.,
1083 Lebrilla, C.B., German, J.B., et al. (2008). The genome sequence of Bifidobacterium longum subsp.

- 1084 infantis reveals adaptations for milk utilization within the infant microbiome. Proceedings of the
1085 National Academy of Sciences *105*, 18964–18969.
- 1086 81. Thomson, P., Medina, D.A., and Garrido, D. (2018). Human milk oligosaccharides and infant gut
1087 bifidobacteria: Molecular strategies for their utilization. *Food Microbiology* *75*, 37–46.
- 1088 82. LoCascio, R.G., Desai, P., Sela, D.A., Weimer, B., and Mills, D.A. (2010). Broad conservation of milk
1089 utilization genes in *Bifidobacterium longum* subsp. *infantis* as revealed by comparative genomic
1090 hybridization. *Appl Environ Microbiol* *76*, 7373–7381.
- 1091 83. Fushinobu, S., and Abou Hachem, M. (2021). Structure and evolution of the bifidobacterial
1092 carbohydrate metabolism proteins and enzymes. *Biochem Soc Trans* *49*, 563–578.
- 1093 84. Wei, X., Guo, Y., Shao, C., Sun, Z., Zhurina, D., Liu, D., Liu, W., Zou, D., Jiang, Z., Wang, X., et al.
1094 (2012). Fructose Uptake in *Bifidobacterium longum* NCC2705 Is Mediated by an ATP-binding
1095 Cassette Transporter. *Journal of Biological Chemistry* *287*, 357–367. 10.1074/jbc.M111.266213.
- 1096 85. Johnstone, T.C., and Nolan, E.M. (2015). Beyond Iron: Non-Classical Biological Functions of
1097 Bacterial Siderophores. *Dalton Trans* *44*, 6320–6339.
- 1098 86. Vazquez-Gutierrez, P., Lacroix, C., Jaeggi, T., Zeder, C., Zimmerman, M.B., and Chassard, C. (2015).
1099 *Bifidobacteria* strains isolated from stools of iron deficient infants can efficiently sequester iron.
1100 *BMC Microbiol* *15*, 3.
- 1101 87. Vazquez-Gutierrez, P., de Wouters, T., Werder, J., Chassard, C., and Lacroix, C. (2016). High Iron-
1102 Sequestering *Bifidobacteria* Inhibit Enteropathogen Growth and Adhesion to Intestinal Epithelial
1103 Cells In vitro. *Front Microbiol* *7*, 1480.
- 1104 88. Gibson, G. r., and Wang, X. (1994). Regulatory effects of bifidobacteria on the growth of other
1105 colonic bacteria. *Journal of Applied Bacteriology* *77*, 412–420.
- 1106 89. Arimond, M., Zeilani, M., Jungjohann, S., Brown, K.H., Ashorn, P., Allen, L.H., and Dewey, K.G.
1107 (2015). Considerations in developing lipid-based nutrient supplements for prevention of
1108 undernutrition: experience from the International Lipid-Based Nutrient Supplements (iLiNS)
1109 Project. *Matern Child Nutr* *11*, 31–61.
- 1110 90. Beal, T., White, J.M., Arsenault, J.E., Okronipa, H., Hinnouho, G.-M., Murira, Z., Torlesse, H., and
1111 Garg, A. (2021). Micronutrient gaps during the complementary feeding period in South Asia: A
1112 Comprehensive Nutrient Gap Assessment. *Nutr Rev* *79*, 26–34.
- 1113 91. White, J.M., Beal, T., Arsenault, J.E., Okronipa, H., Hinnouho, G.-M., Chimanya, K., Matji, J., and
1114 Garg, A. (2021). Micronutrient gaps during the complementary feeding period in 6 countries in
1115 Eastern and Southern Africa: a Comprehensive Nutrient Gap Assessment. *Nutr Rev* *79*, 16–25.
- 1116 92. Park, J.J.H., Harari, O., Siden, E., Dron, L., Zannat, N.-E., Singer, J., Lester, R.T., Thorlund, K., and
1117 Mills, E.J. (2020). Interventions to improve linear growth during complementary feeding period for
1118 children aged 6-24 months living in low- and middle-income countries: a systematic review and
1119 network meta-analysis [version 2; peer review: 3 approved]. *3*, 1660.

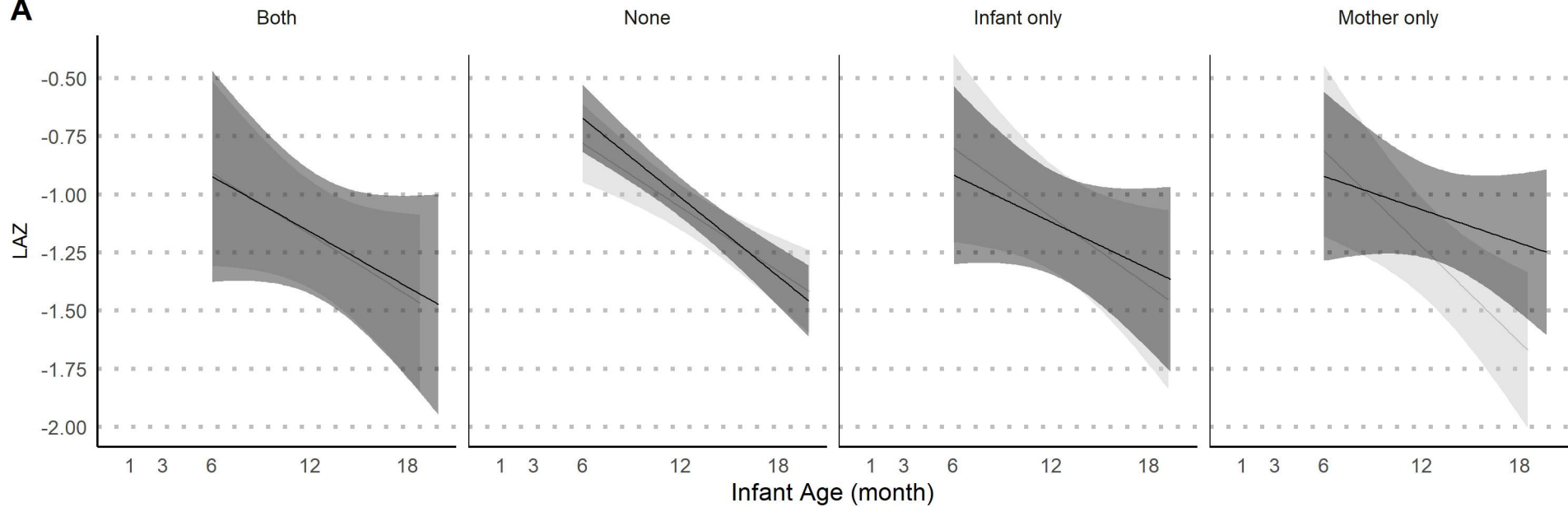
- 1120 93. Imdad, A., and Bhutta, Z.A. (2011). Effect of preventive zinc supplementation on linear growth in
1121 children under 5 years of age in developing countries: a meta-analysis of studies for input to the
1122 lives saved tool. *BMC Public Health* *11*, S22.
- 1123 94. Ashorn, P., Alho, L., Ashorn, U., Cheung, Y.B., Dewey, K.G., Gondwe, A., Harjunmaa, U., Lartey, A.,
1124 Phiri, N., Phiri, T.E., et al. (2015). Supplementation of Maternal Diets during Pregnancy and for 6
1125 Months Postpartum and Infant Diets Thereafter with Small-Quantity Lipid-Based Nutrient
1126 Supplements Does Not Promote Child Growth by 18 Months of Age in Rural Malawi: A Randomized
1127 Controlled Trial. *J Nutr* *145*, 1345–1353. 10.3945/jn.114.207225.
- 1128 95. Abellan-Schneyder, I., Matchado, M.S., Reitmeier, S., Sommer, A., Sewald, Z., Baumbach, J., List,
1129 M., and Neuhaus, K. (2021). Primer, Pipelines, Parameters: Issues in 16S rRNA Gene Sequencing.
1130 *mSphere* *6*, e01202-20.
- 1131 96. Paganini, D., Uyoga, M.A., Kortman, G.A.M., Boekhorst, J., Schneeberger, S., Karanja, S., Henet, T.,
1132 and Zimmermann, M.B. (2019). Maternal Human Milk Oligosaccharide Profile Modulates the
1133 Impact of an Intervention with Iron and Galacto-Oligosaccharides in Kenyan Infants. *Nutrients* *11*,
1134 2596.
- 1135 97. Schwartz, D.J., Langdon, A., Sun, X., Langendorf, C., Berthé, F., Grais, R.F., Trehan, I., Isanaka, S.,
1136 and Dantas, G. (2023). Effect of amoxicillin on the gut microbiome of children with severe acute
1137 malnutrition in Madarounfa, Niger: a retrospective metagenomic analysis of a placebo-controlled
1138 trial. *The Lancet Microbe* *4*, e931–e942.
- 1139 98. Ruiz, L., Flórez, A.B., Sánchez, B., Moreno-Muñoz, J.A., Rodríguez-Palmero, M., Jiménez, J., Gavilán,
1140 C.G. de los R., Gueimonde, M., Ruas-Madiedo, P., and Margolles, A. (2020). *Bifidobacterium*
1141 *longum* subsp. *infantis* CECT7210 (*B. infantis* IM-1®) Displays In Vitro Activity against Some
1142 Intestinal Pathogens. *Nutrients* *12*, 3259.
- 1143 99. Henrick, B.M., Rodriguez, L., Lakshmikanth, T., Pou, C., Henckel, E., Arzoomand, A., Olin, A., Wang,
1144 J., Mikes, J., Tan, Z., et al. (2021). *Bifidobacteria*-mediated immune system imprinting early in life.
1145 *Cell* *184*, 3884-3898.e11.
- 1146 100. Dai, D.L.Y., Petersen, C., Hoskinson, C., Del Bel, K.L., Becker, A.B., Moraes, T.J., Mandhane, P.J.,
1147 Finlay, B.B., Simons, E., Kozyrskyj, A.L., et al. (2023). Breastfeeding enrichment of *B. longum* subsp.
1148 *infantis* mitigates the effect of antibiotics on the microbiota and childhood asthma risk. *Med* *4*, 92-
1149 112.e5.
- 1150 101. Barratt, M.J., Nuzhat, S., Ahsan, K., Frese, S.A., Arzamasov, A.A., Sarker, S.A., Islam, M.M., Palit, P.,
1151 Islam, M.R., Hibberd, M.C., et al. (2022). *Bifidobacterium infantis* treatment promotes weight gain
1152 in Bangladeshi infants with severe acute malnutrition. *Sci Transl Med* *14*, eabk1107.
- 1153 102. Nuzhat, S., Hasan, S.M.T., Palit, P., Islam, M.R., Mahfuz, M., Islam, M.M., Alam, M.A., Flannery, R.L.,
1154 Kyle, D.J., Sarker, S.A., et al. (2023). Effects of probiotic and synbiotic supplementation on ponderal
1155 and linear growth in severely malnourished young infants in a randomized clinical trial. *Sci Rep* *13*,
1156 1845.
- 1157 103. Humphrey, J.H., Jones, A.D., Manges, A., Mangwadu, G., Maluccio, J.A., Mbuya, M.N.N., Moulton,
1158 L.H., Ntozini, R., Prendergast, A.J., Stoltzfus, R.J., et al. (2015). The sanitation hygiene infant

- 1159 nutrition efficacy (SHINE) Trial: Rationale, design, and methods. *Clinical Infectious Diseases* 61,
1160 S685-702.
- 1161 104. Chasekwa, B., Maluccio, J.A., Ntozini, R., Moulton, L.H., Wu, F., Smith, L.E., Matare, C.R., Stoltzfus,
1162 R.J., Mbuya, M.N.N., Tielsch, J.M., et al. (2018). Measuring wealth in rural communities: Lessons
1163 from the sanitation, hygiene, infant nutrition efficacy (SHINE) trial. *PLoS ONE* 13, 1–19.
- 1164 105. Maxwell, D., Watkins, B., Wheeler, R., and Collins, G. (2003). The Coping Strategy Index: a tool for
1165 rapid measurement of household food security and the impact of food aid programs in
1166 humanitarian emergencies. (*CARE and WFP*).
- 1167 106. E.K, G., L.H, M., K, M., R, N., R.J, S., F.D, M., L.E, S., G, P., N, G., M, J., et al. (2020). Effects of
1168 improved water, sanitation, and hygiene and improved complementary feeding on environmental
1169 enteric dysfunction in children in rural Zimbabwe: A cluster-randomized controlled trial. *PLoS*
1170 *Neglected Tropical Diseases* 14, e0007963.
- 1171 107. Mutasa, K., Ntozini, R., Mbuya, M.N.N., Rukobo, S., Govha, M., Majo, F.D., Tavengwa, N., Smith,
1172 L.E., Caulfield, L., Swann, J.R., et al. (2021). Biomarkers of environmental enteric dysfunction are
1173 not consistently associated with linear growth velocity in rural Zimbabwean infants. *The American*
1174 *journal of clinical nutrition* 113.
- 1175 108. Colston, J.M., Francois, R., Pisanic, N., Yori, P.P., McCormick, B.J.J., Olortegui, M.P., Gazi, M.A.,
1176 Svensen, E., Ahmed, M.M.M., Mduma, E., et al. (2019). Effects of Child and Maternal Histo-Blood
1177 Group Antigen Status on Symptomatic and Asymptomatic Enteric Infections in Early Childhood.
1178 *Journal of Infectious Diseases* 220, 151–162.
- 1179 109. Legendre, P., and Anderson, M.J. (1999). Distance-Based Redundancy Analysis: Testing
1180 Multispecies Responses in Multifactorial Ecological Experiments. *Ecological Monographs* 69, 1–24.
- 1181 110. Anderson, M.J. (2001). A new method for non-parametric multivariate analysis of variance. *Austral*
1182 *Ecology* 26, 32–46.
- 1183 111. VanderWeele, T.J. (2012). Sample Size and Power Calculations for Additive Interactions. *Epidemiol*
1184 *Methods* 1, 159–188.
- 1185 112. Naimi, A.I., and Whitcomb, B.W. (2020). Estimating Risk Ratios and Risk Differences Using
1186 Regression. *Am J Epidemiol* 189, 508–510.
- 1187 113. Benjamini, Y., and Hochberg, Y. (1995). Controlling the False Discovery Rate: A Practical and
1188 Powerful Approach to Multiple Testing. *Journal of the Royal Statistical Society. Series B*
1189 *(Methodological)* 57, 289–300.
- 1190 114. Scholz, M., Ward, D.V., Pasolli, E., Tolio, T., Zolfo, M., Asnicar, F., Truong, D.T., Tett, A., Morrow,
1191 A.L., and Segata, N. (2016). Strain-level microbial epidemiology and population genomics from
1192 shotgun metagenomics. *Nature Methods* 13, 435–438.
- 1193 115. Murtagh, F., and Legendre, P. (2014). Ward’s Hierarchical Agglomerative Clustering Method:
1194 Which Algorithms Implement Ward’s Criterion? *Journal of Classification* 31, 274–295.

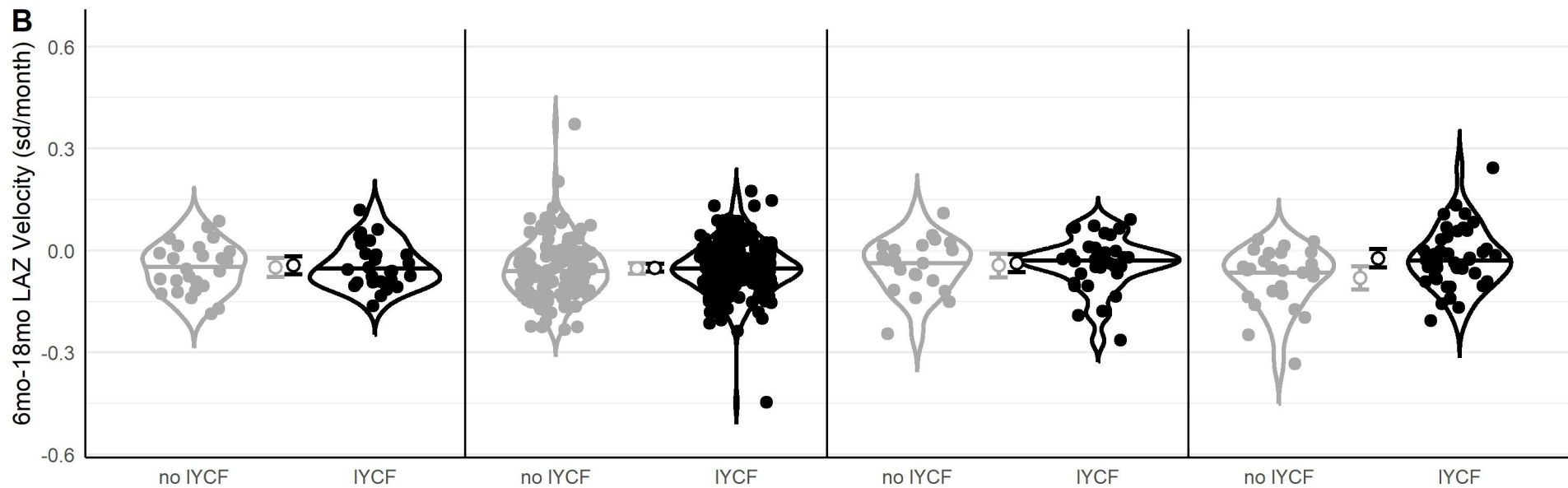
- 1195 116. Chen, E.Z., and Li, H. (2016). A two-part mixed-effects model for analyzing longitudinal microbiome
1196 compositional data. In *Bioinformatics*, pp. 2611–2617. 10.1093/bioinformatics/btw308.
- 1197 117. Kosmidis, I., Kenne Pagui, E.C., and Sartori, N. (2020). Mean and median bias reduction in
1198 generalized linear models. *Stat Comput* 30, 43–59.
- 1199 118. Mansournia, M.A., Geroldinger, A., Greenland, S., and Heinze, G. (2018). Separation in Logistic
1200 Regression: Causes, Consequences, and Control. *Am J Epidemiol* 187, 864–870.
- 1201 119. Dixon, P. (2003). VEGAN, a package of R functions for community ecology. *Journal of Vegetation*
1202 *Science* 14, 927–930.
- 1203 120. Stasinopoulos, D.M., and Rigby, R.A. (2007). Generalized additive models for location scale and
1204 shape (GAMLSS) in R. *Journal of Statistical Software* 23, 1–46. 10.18637/jss.v023.i07.
- 1205
- 1206

no IYCF IYCF

A

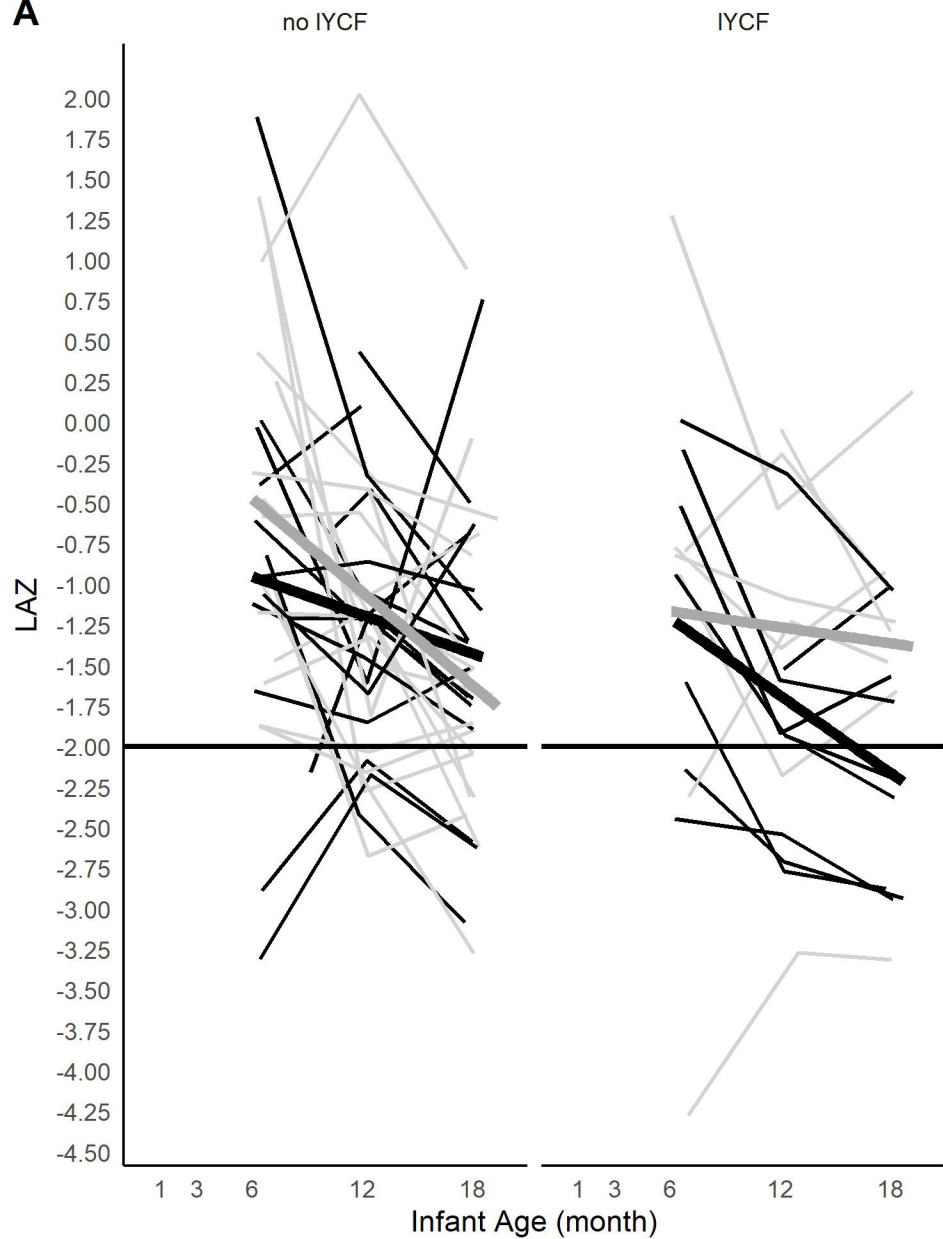


B

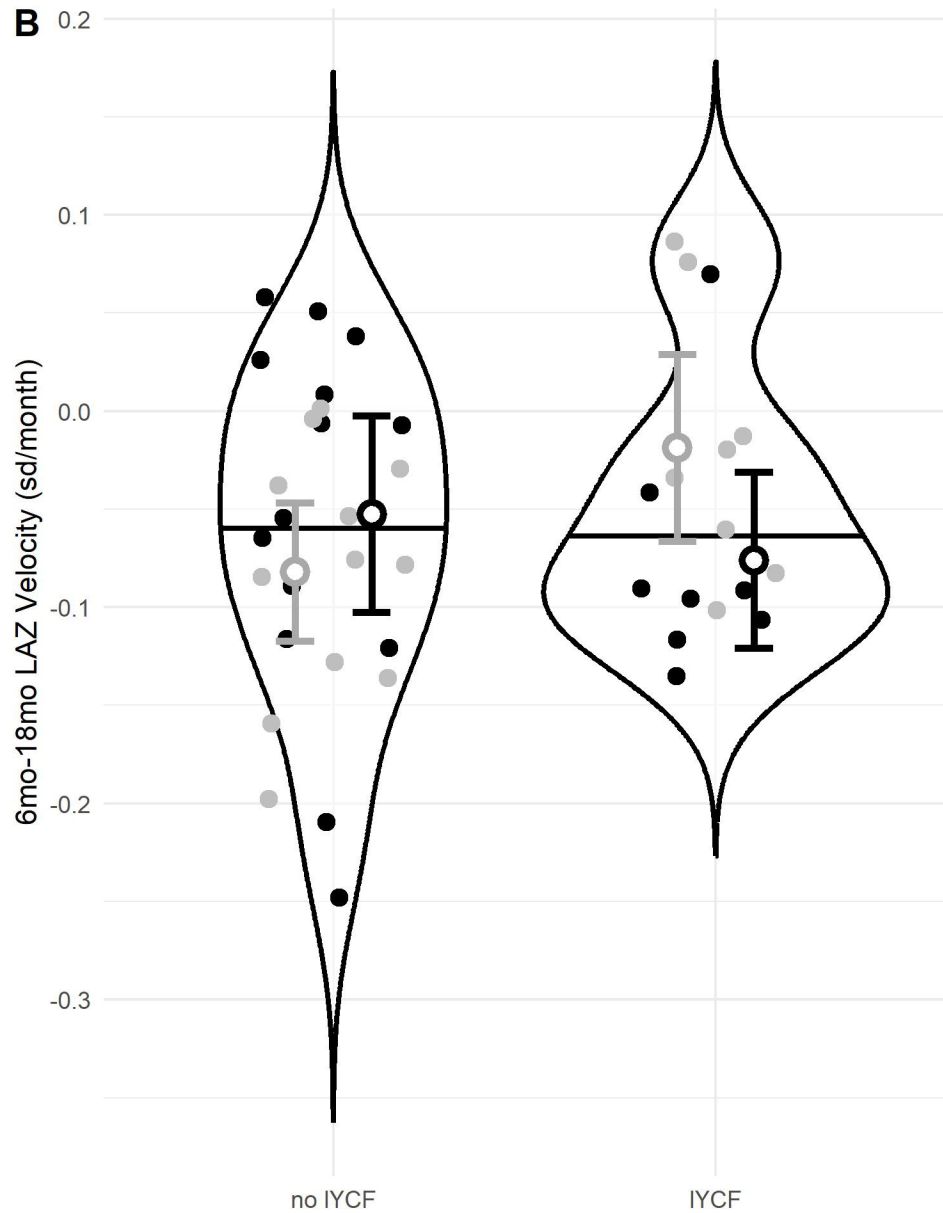


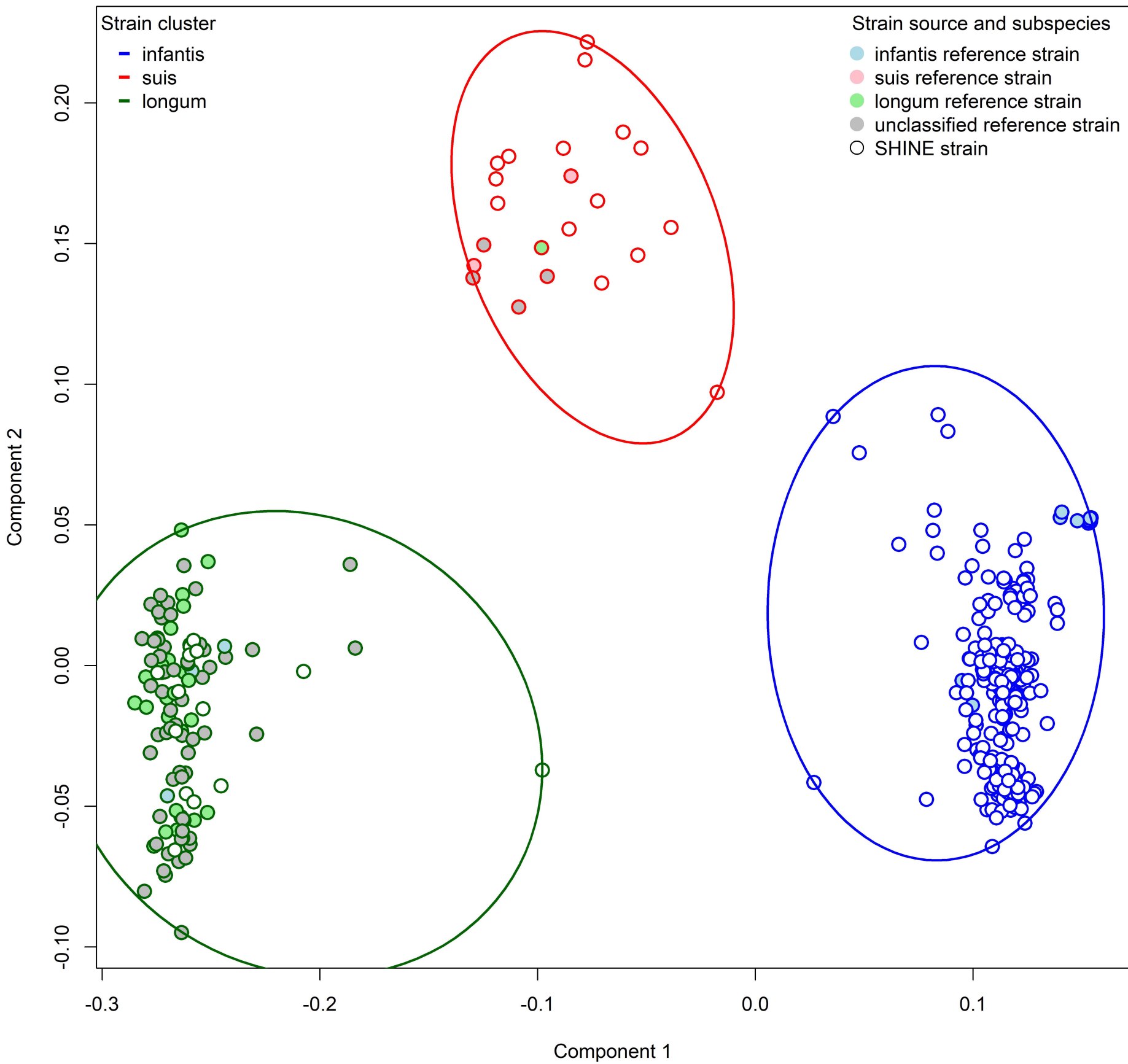
B. longum Rel. Ab. — Low — High

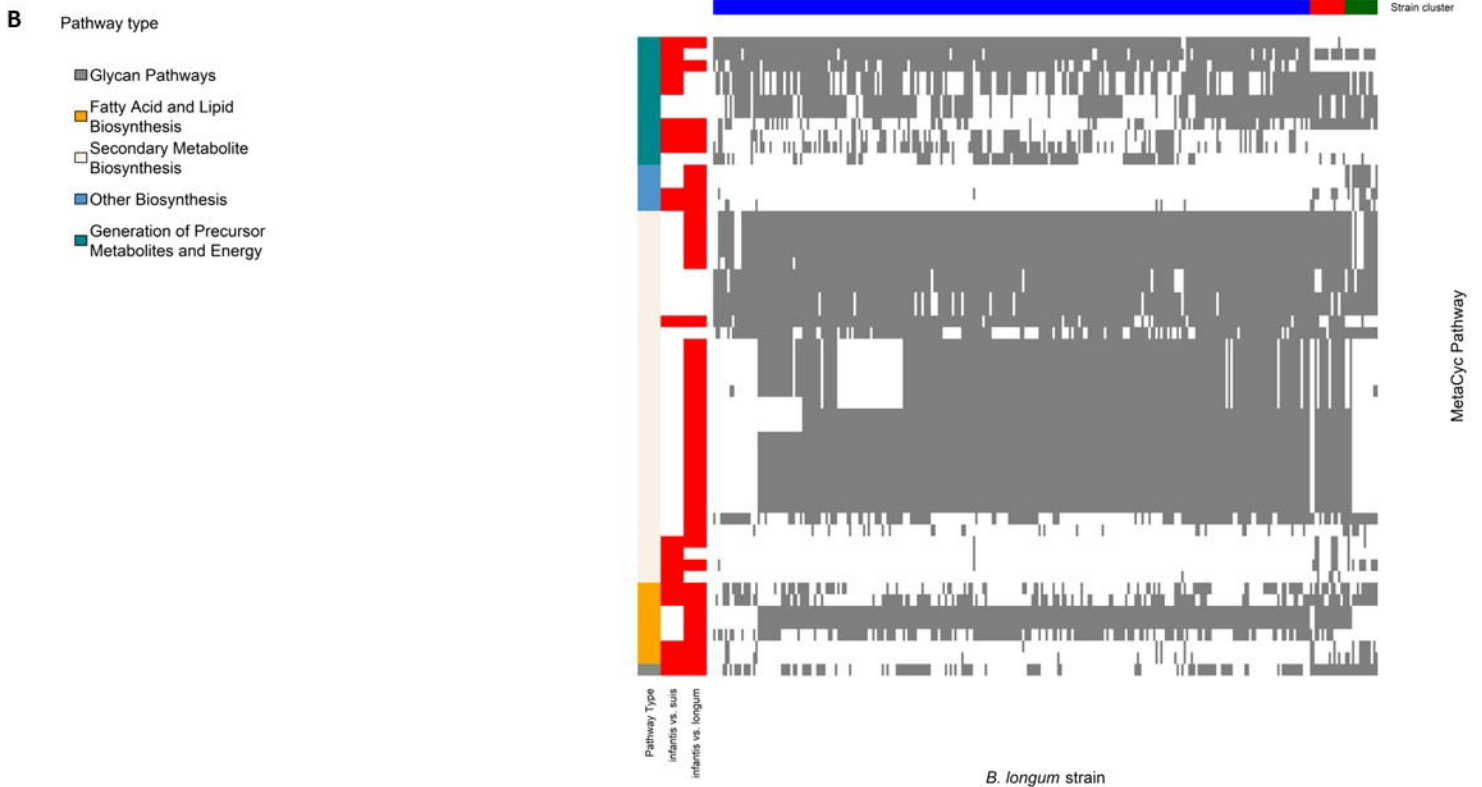
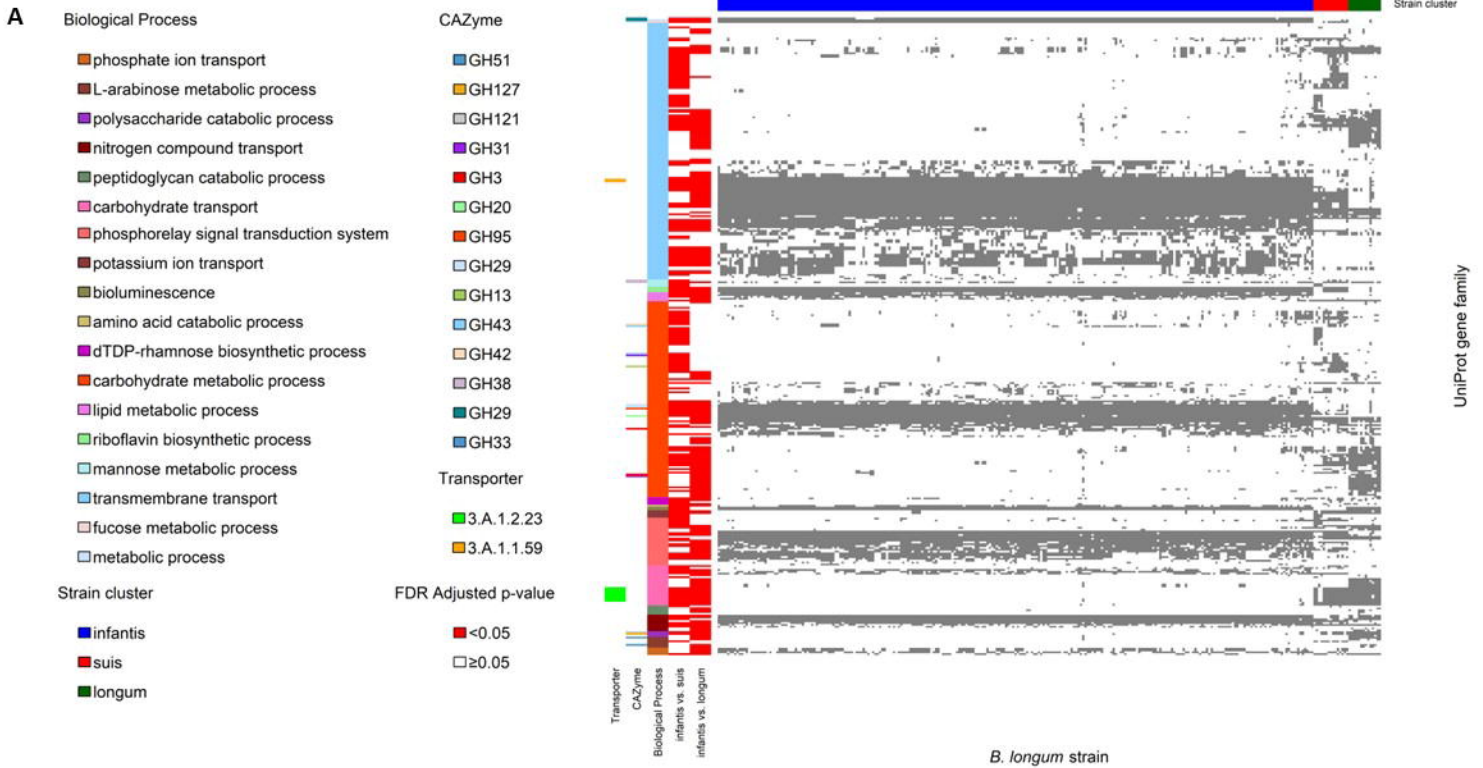
A



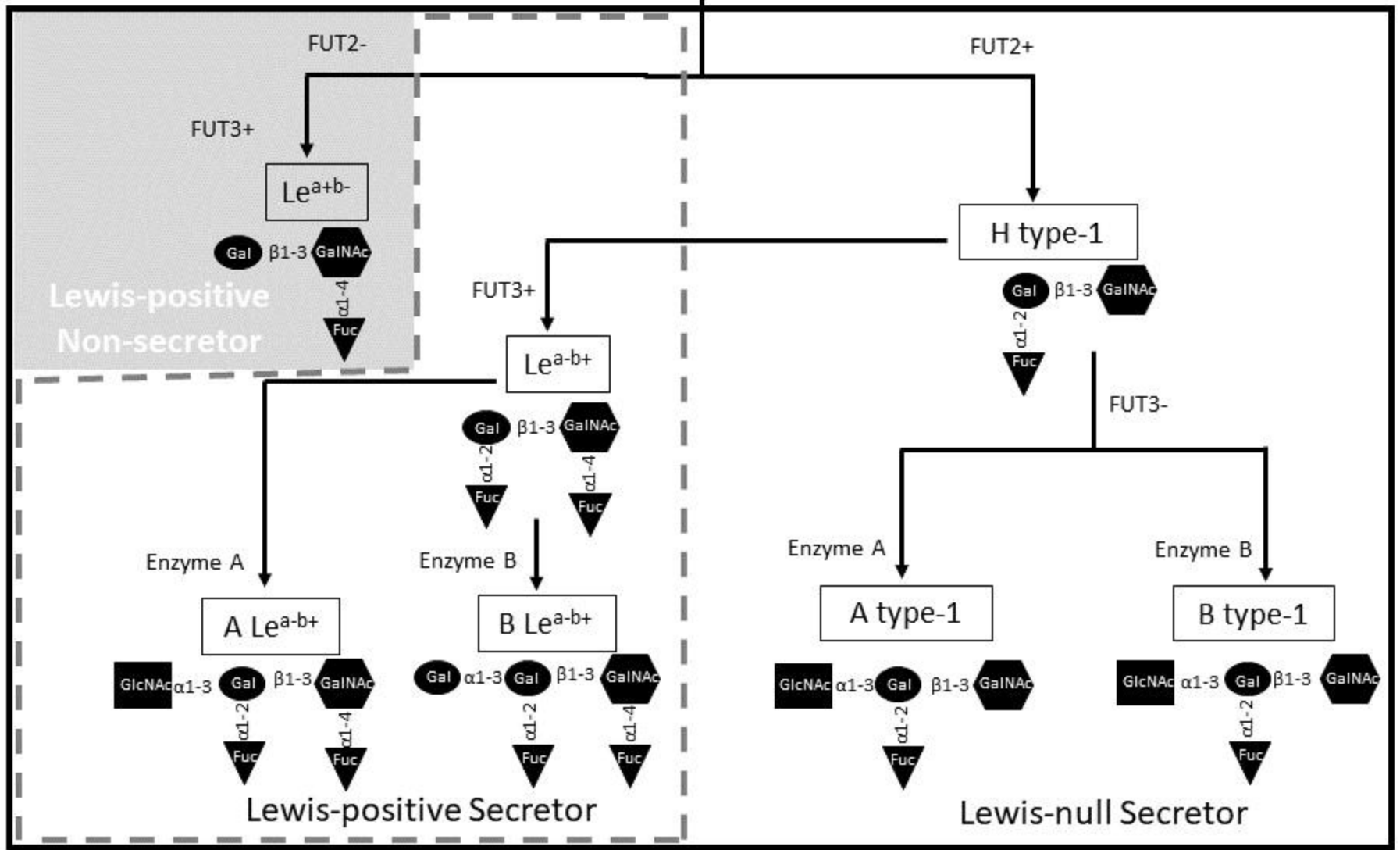
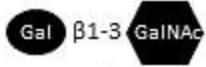
B





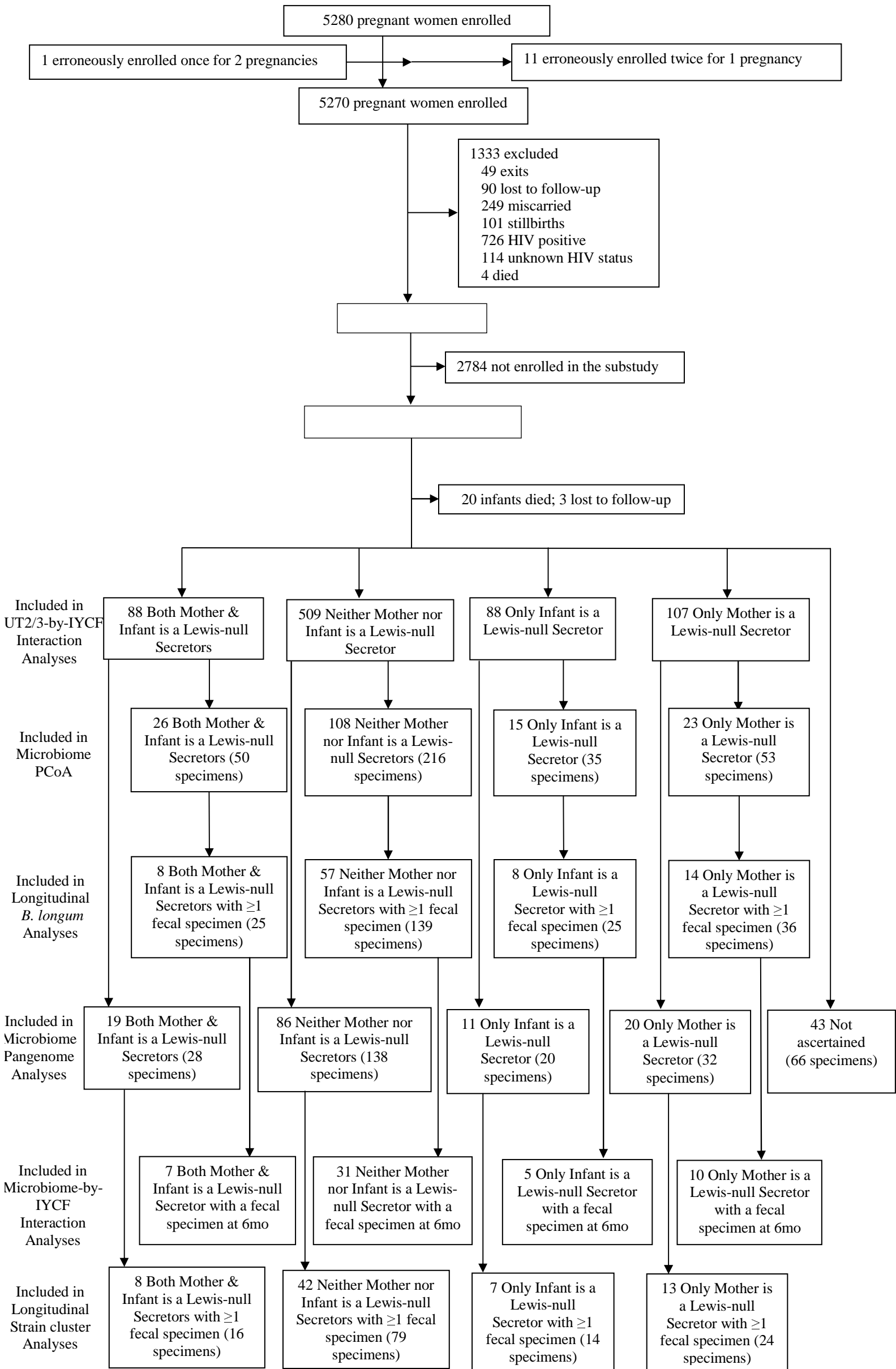


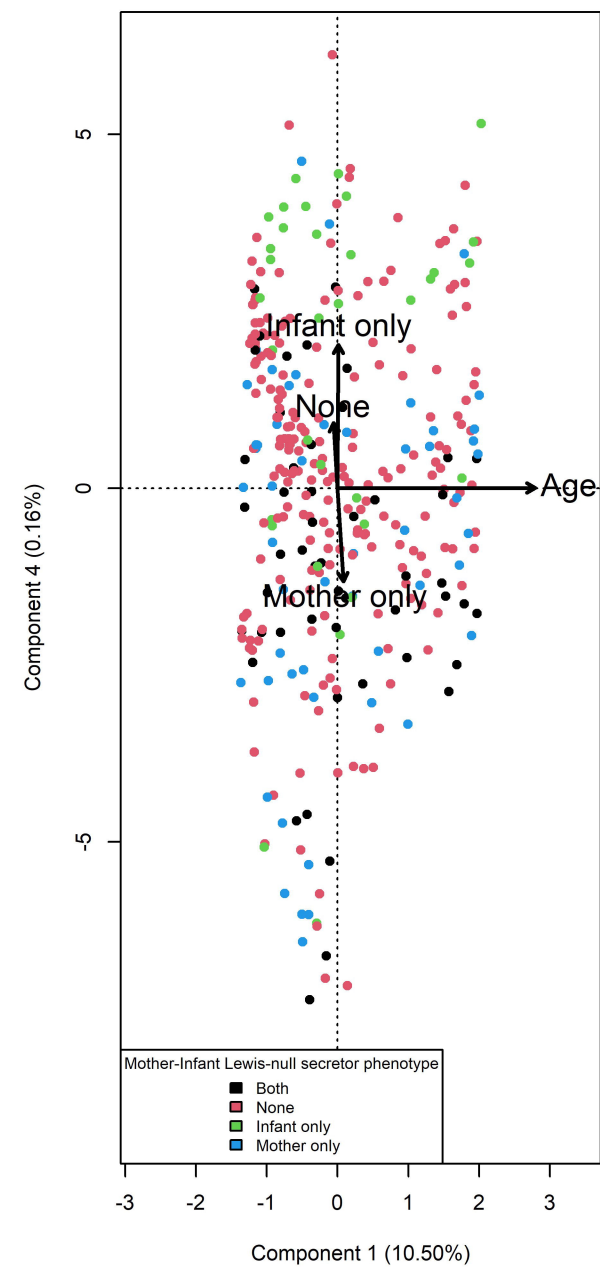
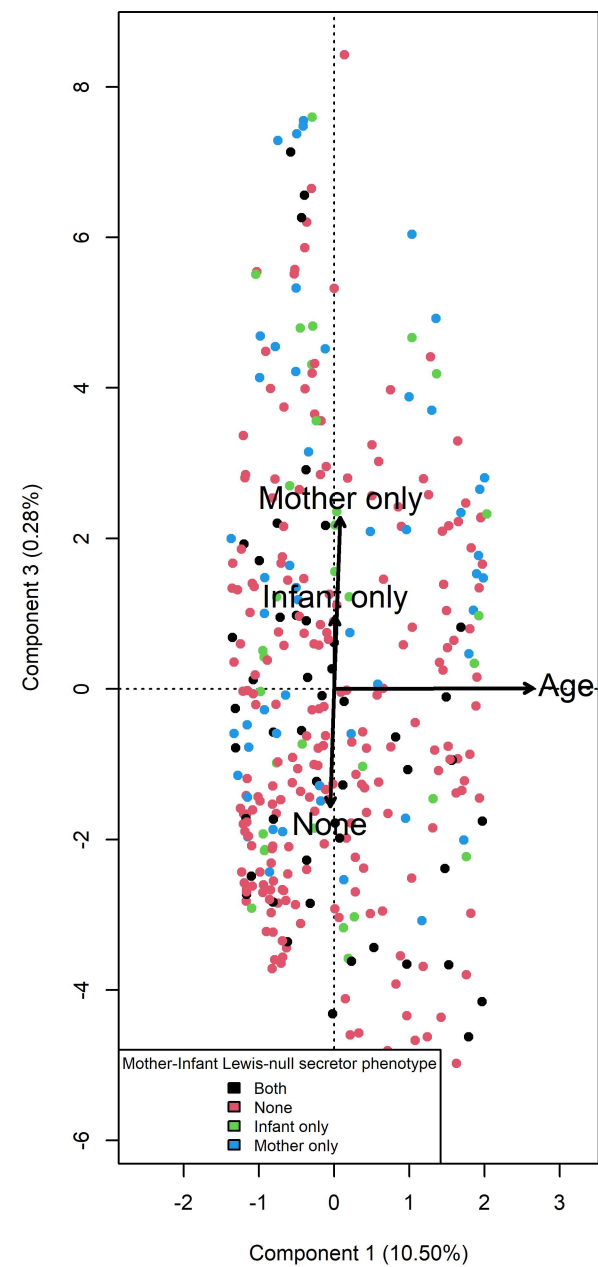
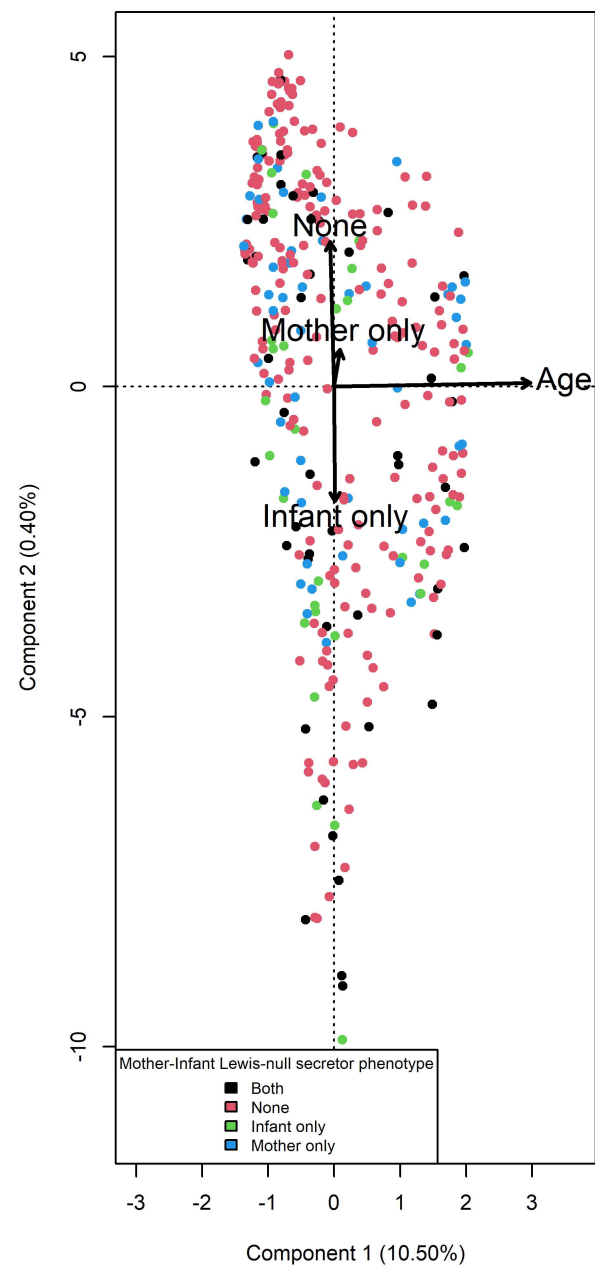
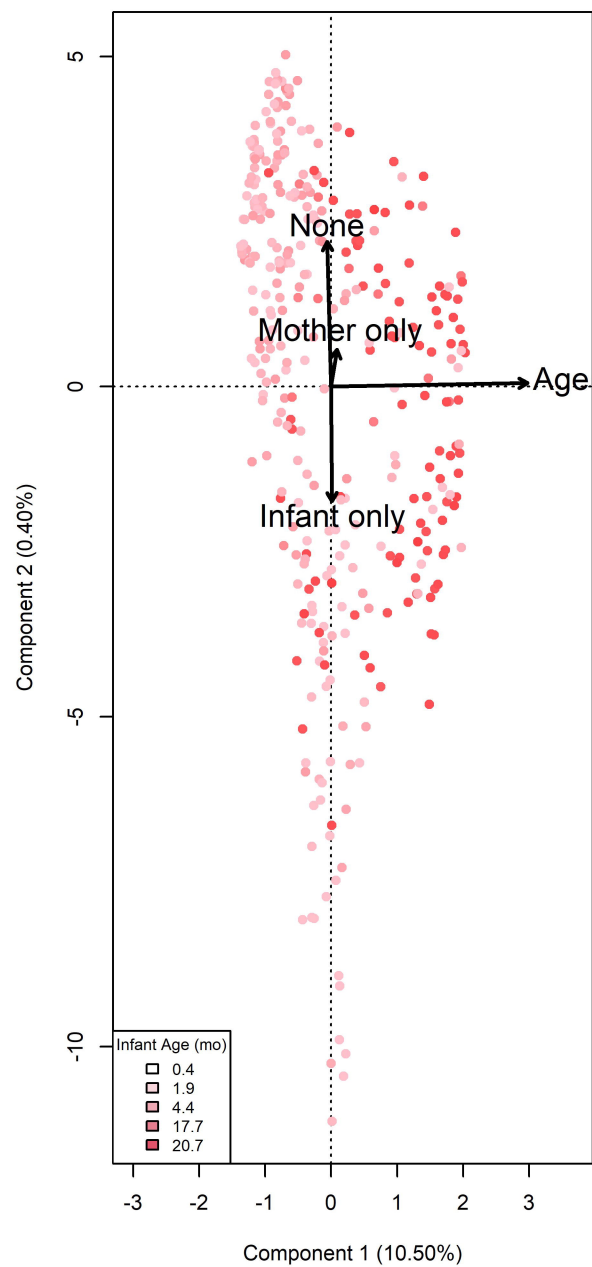
Type 1 Precursor

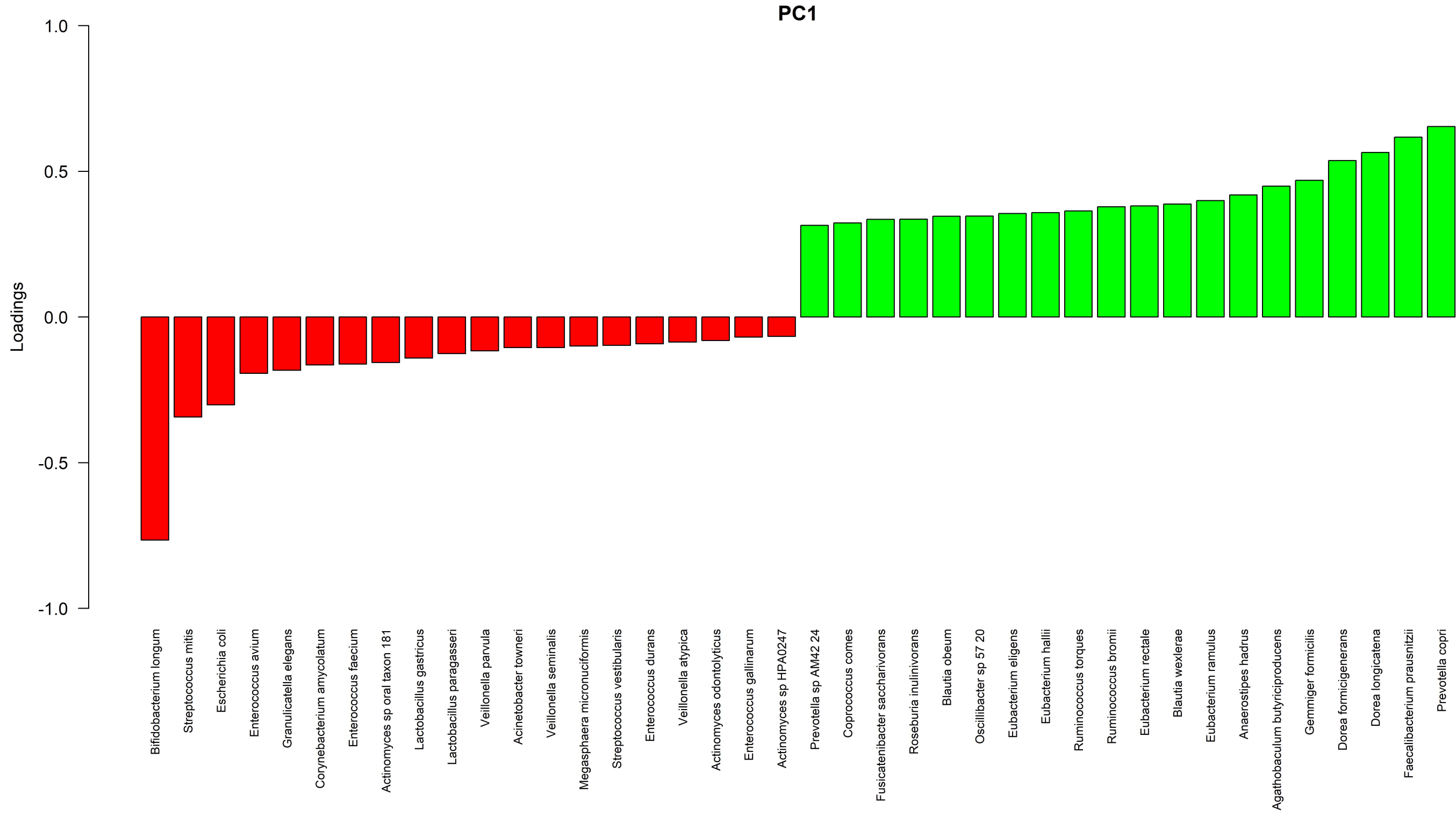


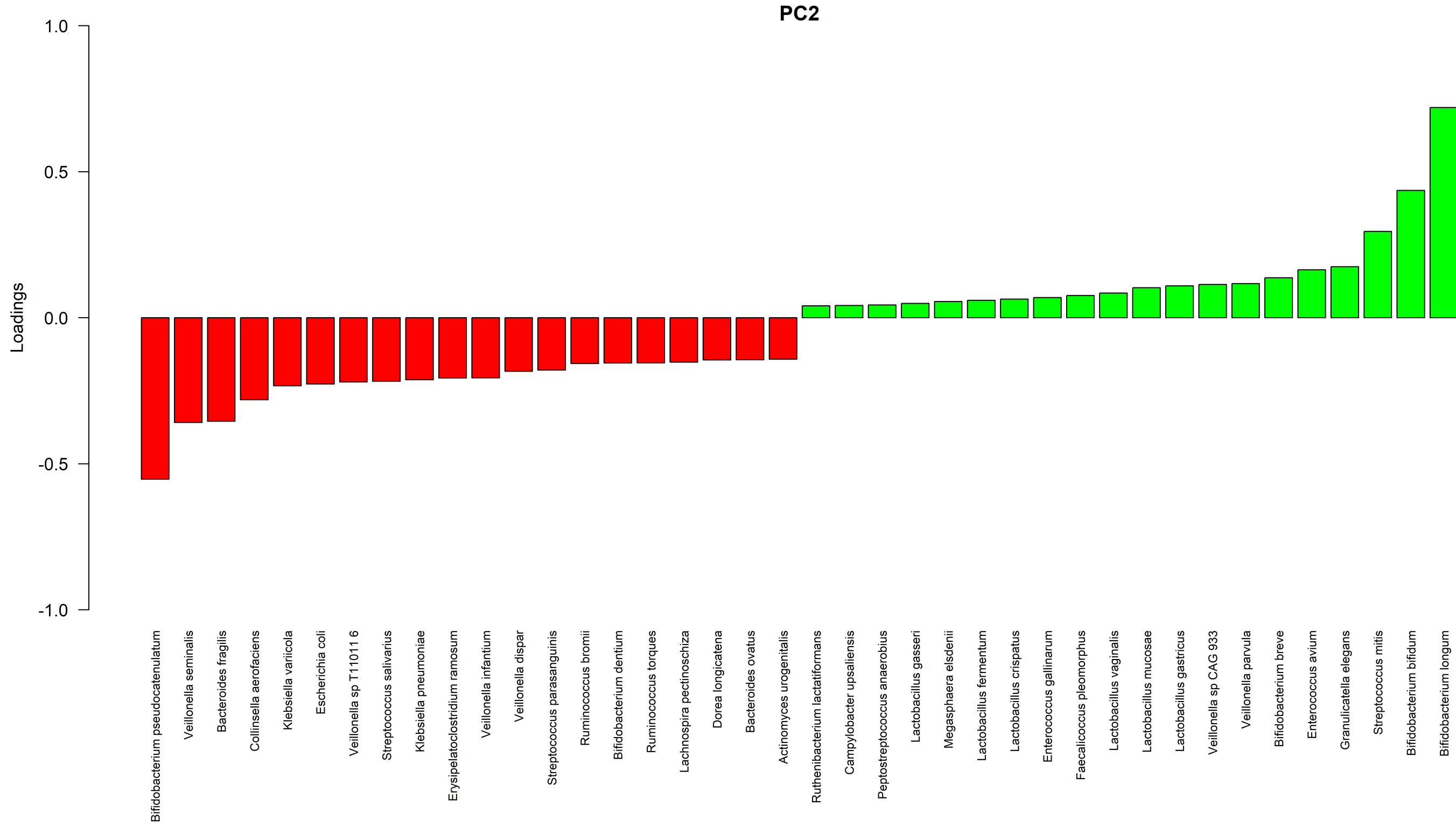
Legend:

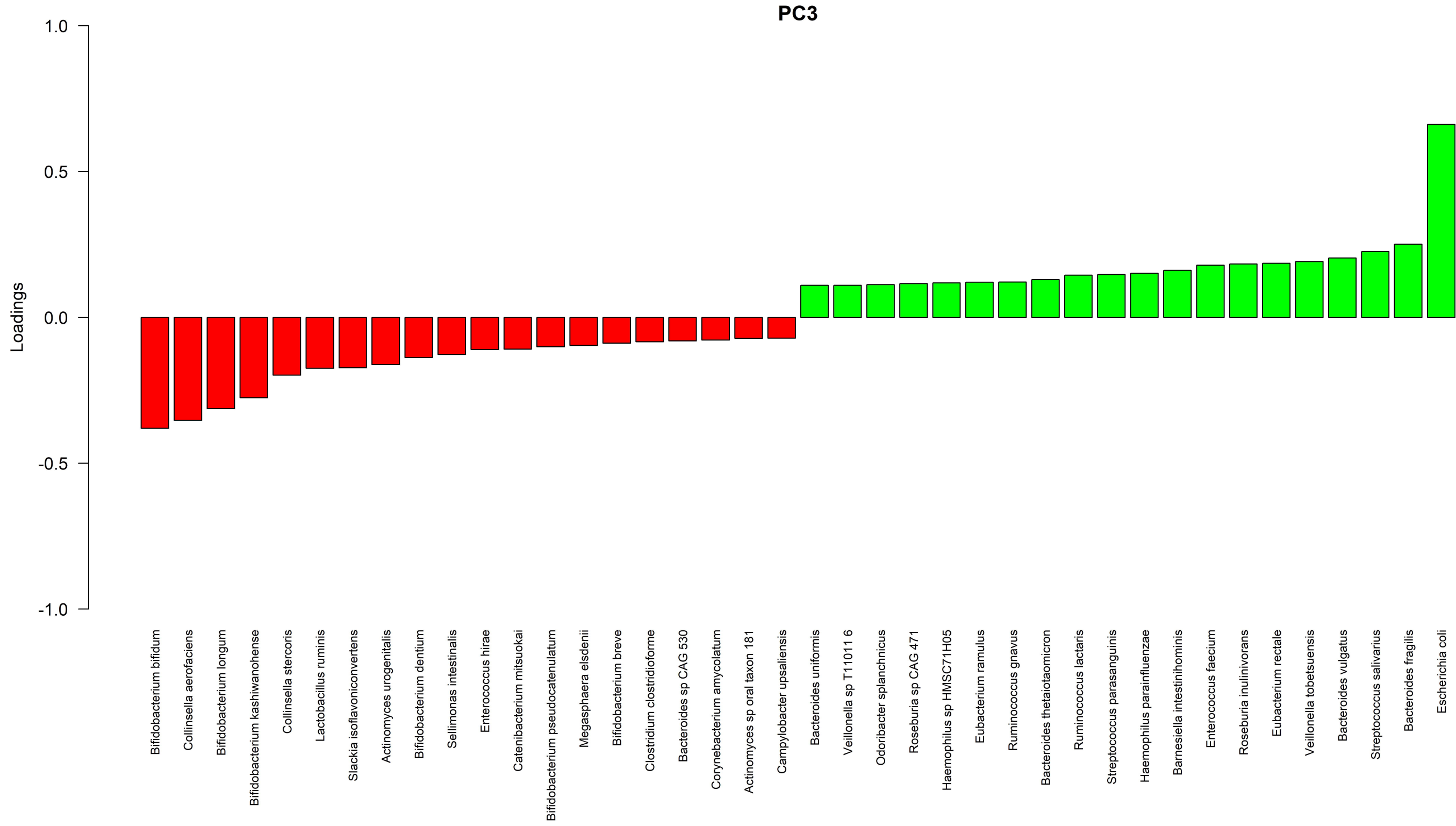
- Gal: Galactose
- Fuc: Fucose
- GlcNAc: N-Acetyl Glucosamine
- GalNAc: N-Acetyl Galactosamine

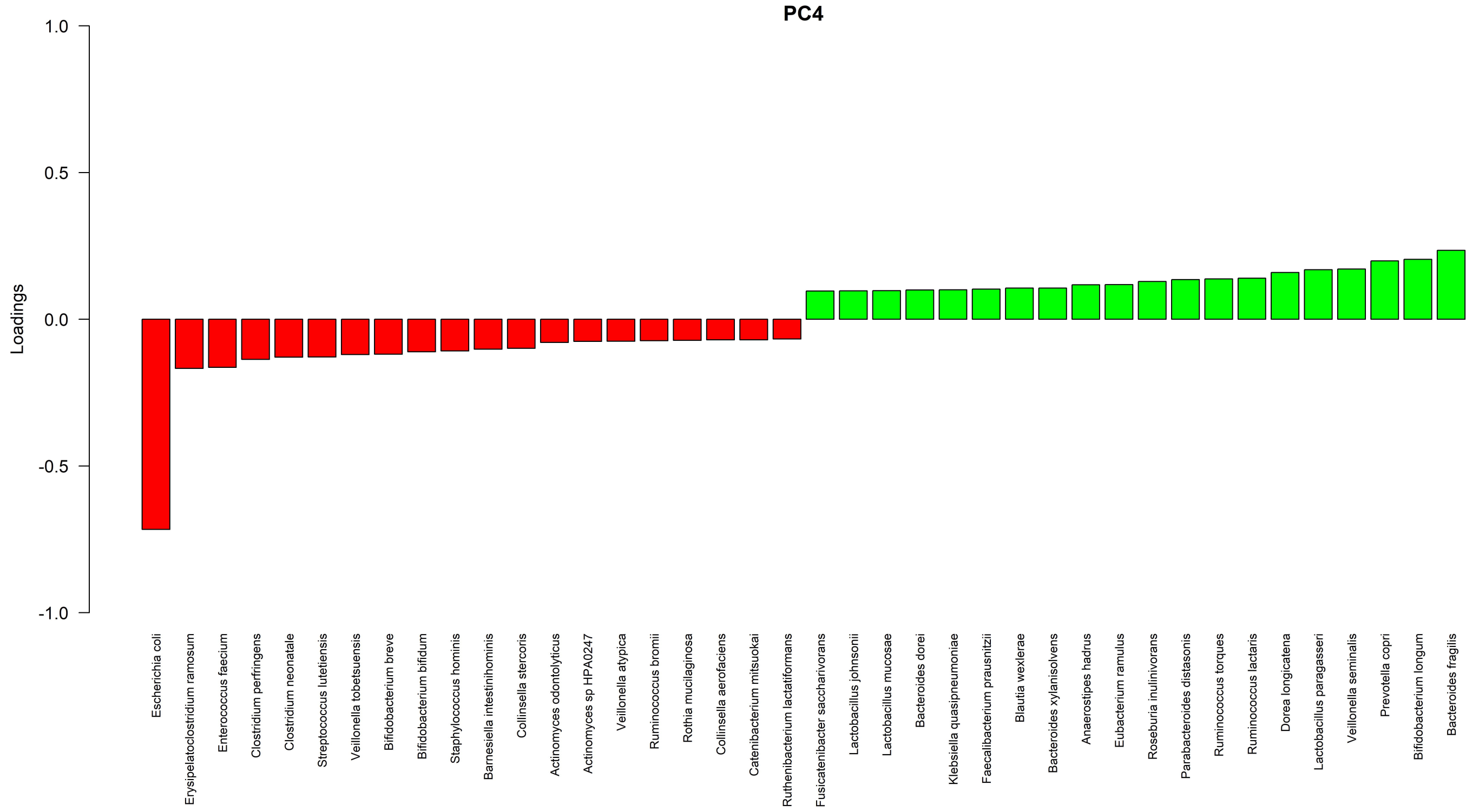












Reference subspecies

- longum
- infantis
- suis
- unclassified

Strain cluster

- infants
- suis
- longum

Strain source

- Reference strain
- SHINE strain

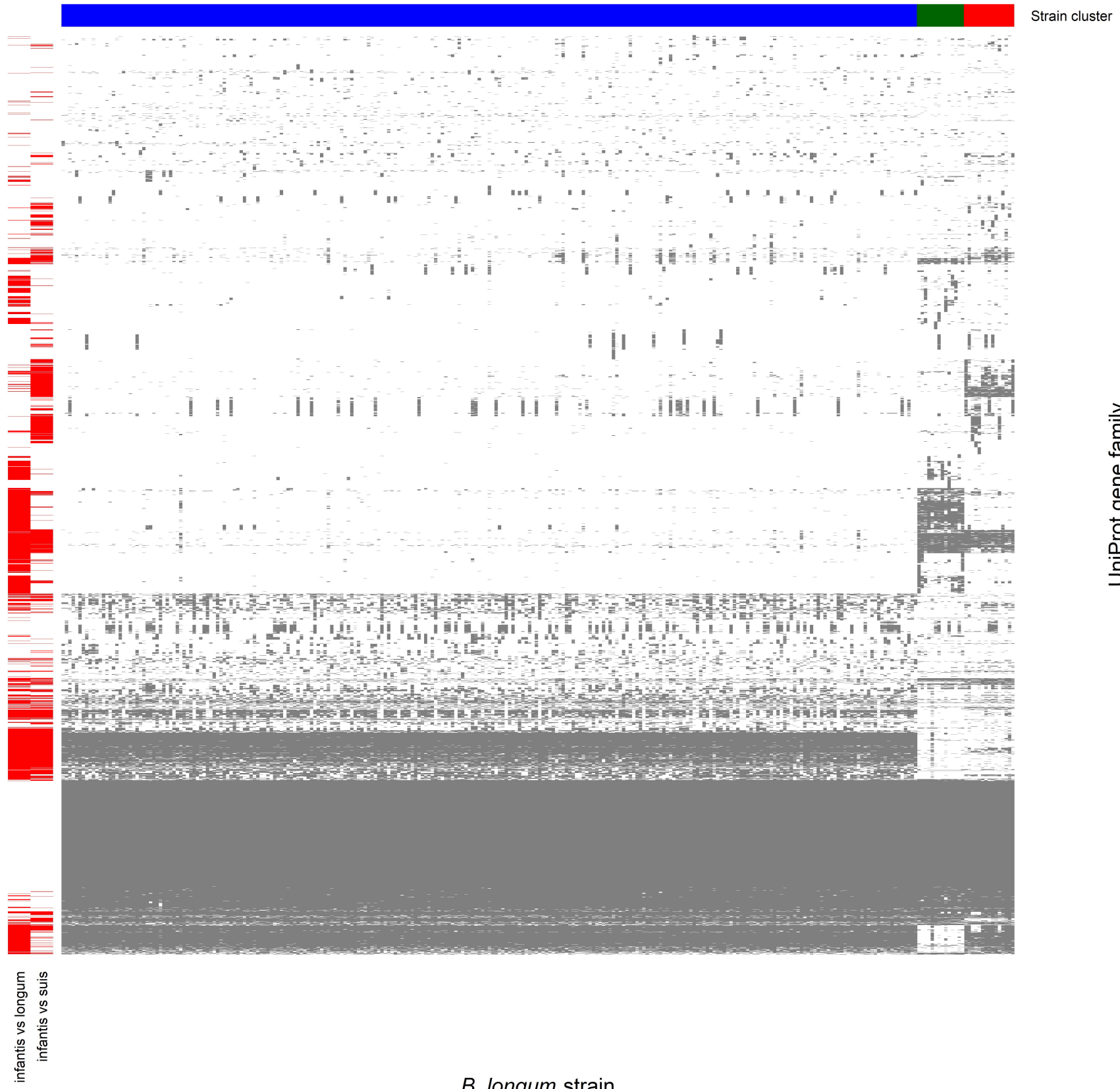
Strain source
Reference subspecies
Strain cluster



B. longum strain

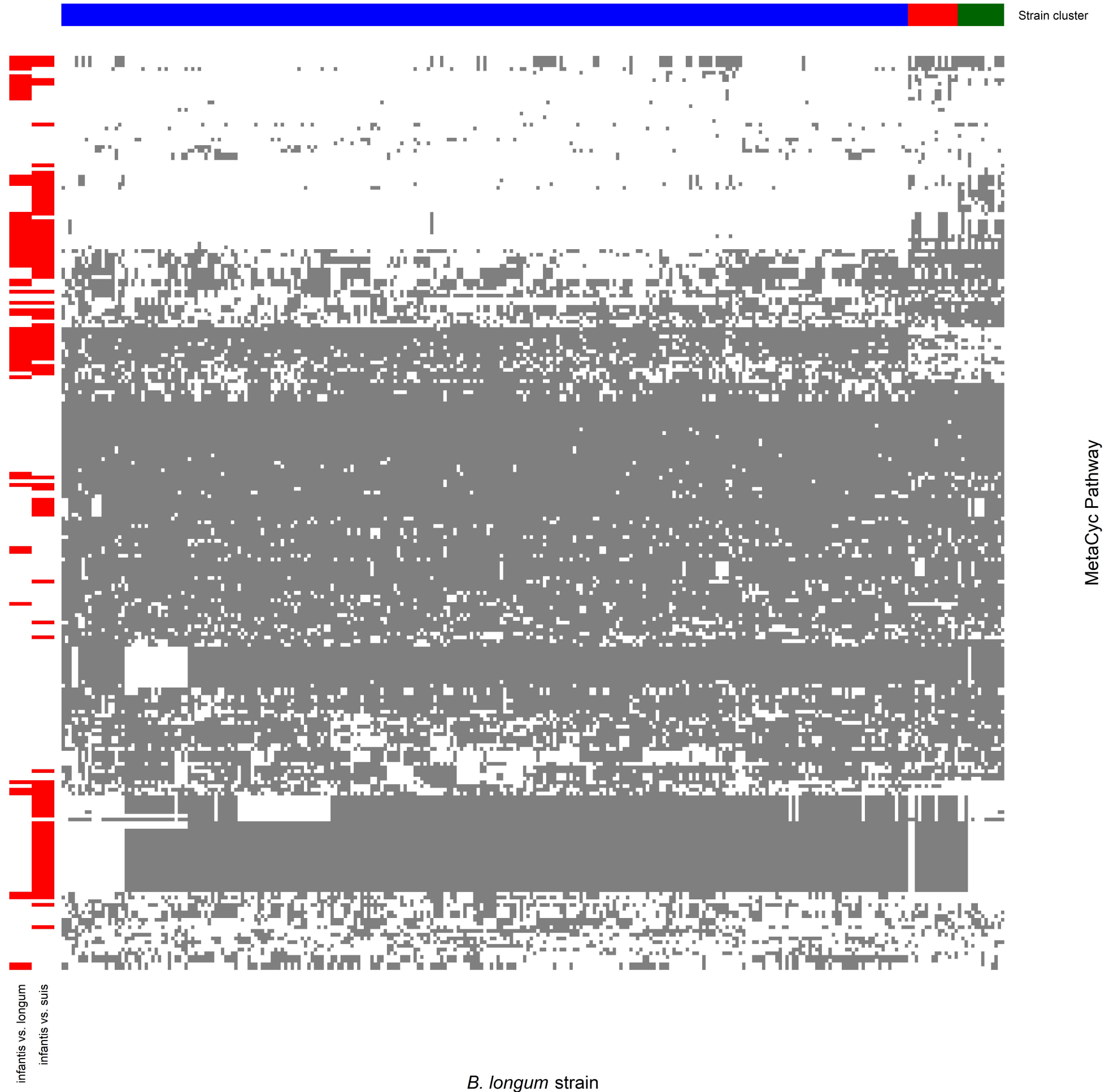
FDR Adjusted p-value
■ <0.05
□ ≥0.05

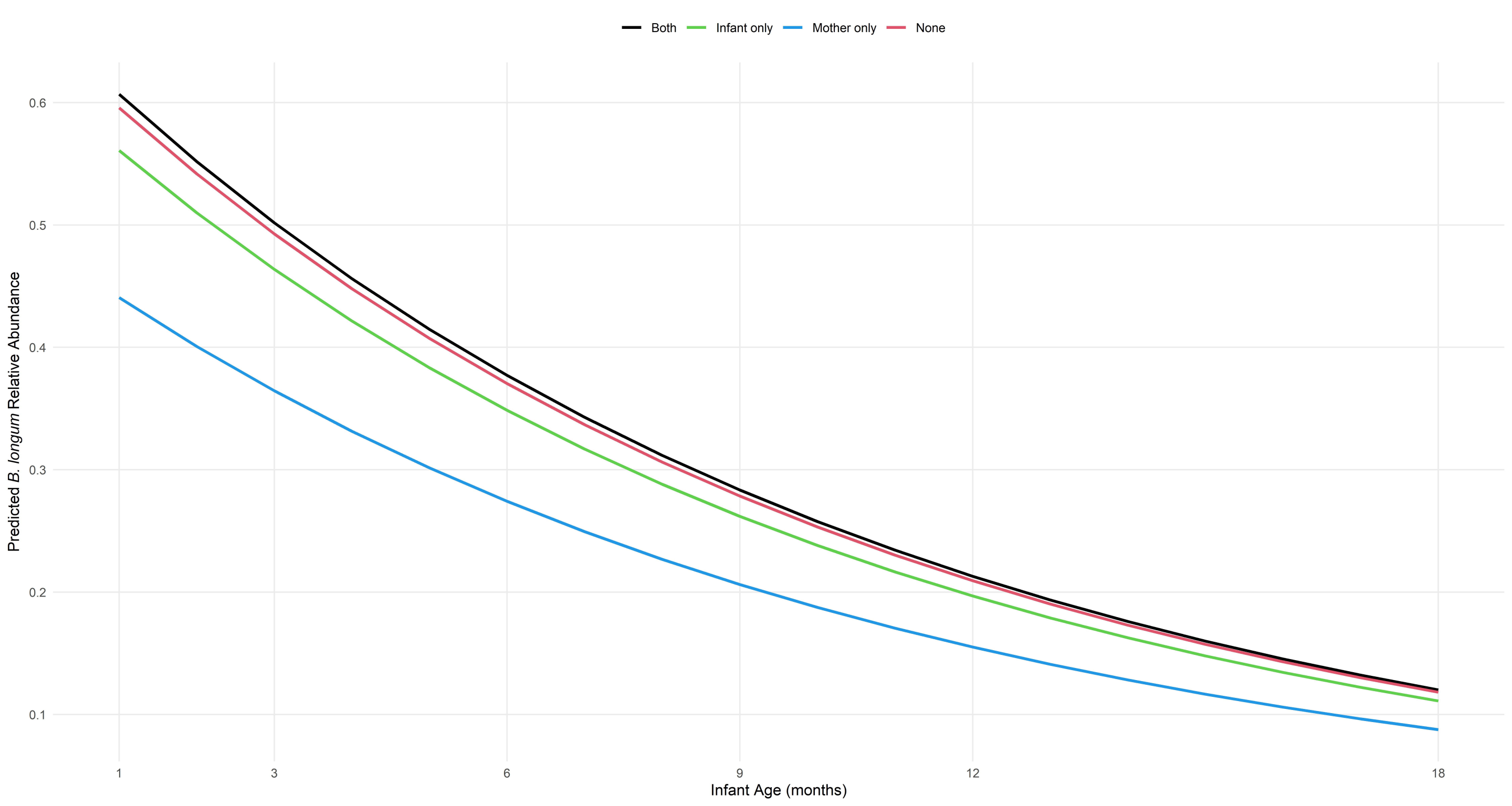
Strain cluster
■ infantis
■ suis
■ longum

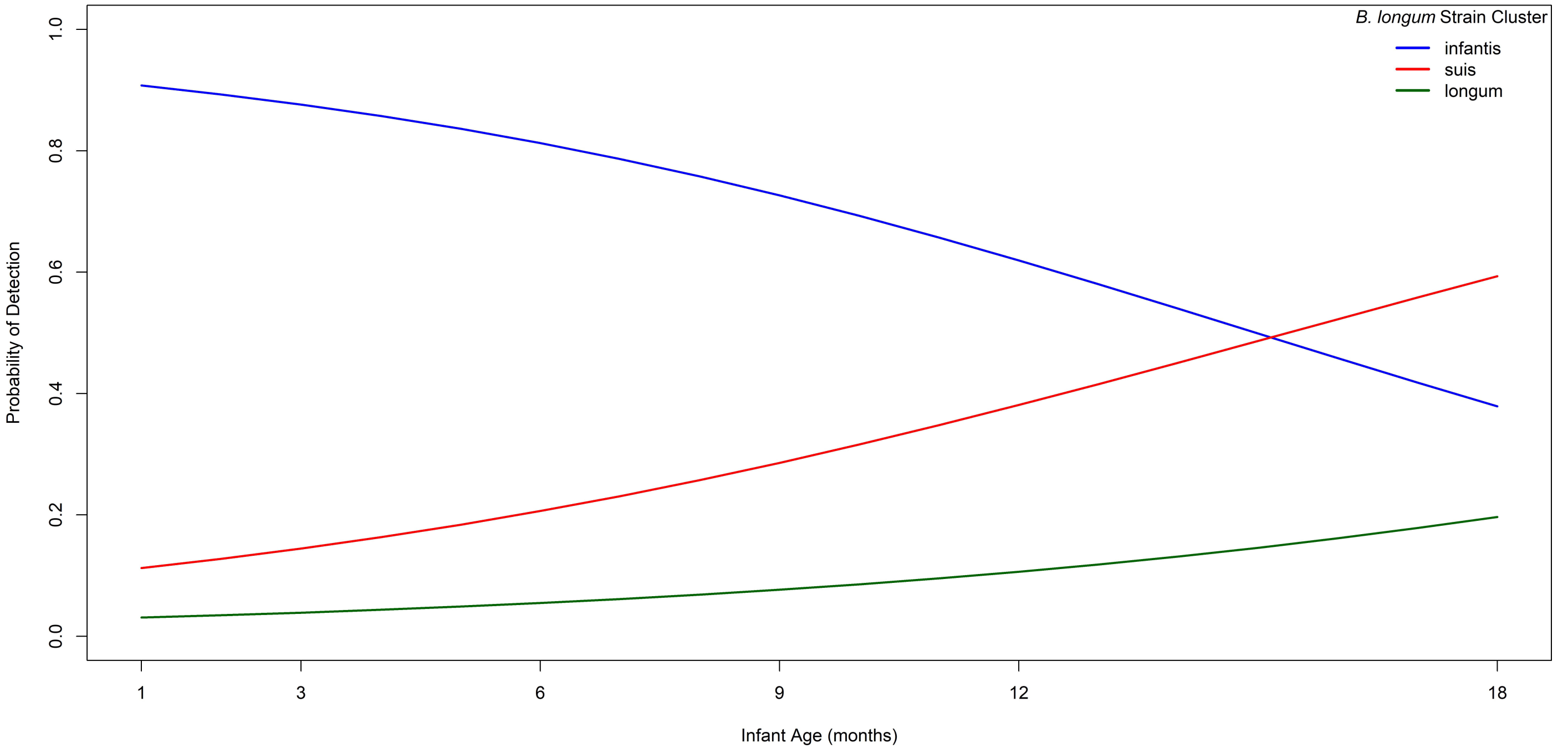


FDR Adjusted p-value
■ <0.05
□ ≥0.05

Strain cluster
■ infantis
■ suis
■ longum







— Both — None — Infant only — Mother only

